Report 2138

THE EFFECT OF SHORT-PULSE LASER RADIATION ON COATINGS

April 1975

Approved for public release; distribution unlimited.

U.S. ARMY MOBILITY EQUIPMENT RESEARCH AND DEVELOPMENT CENTER
FORT BELVOIR, VIRGINIA

UNCLASSIFIED

SECURITY CLASSIFICATION OF THIS PAGE (When Data Entered)

REPORT DOCUMENTATION PAGE		READ INSTRUCTIONS BEFORE COMPLETING FORM
1. REPORT NUMBER 2138	2. GOVT ACCESSION NO.	3. RECIPIENT'S CATALOG NUMBER
4. TITLE (and Subtitle) THE EFFECT OF SHORT-PULSE LASER RADIATION ON COATINGS		5. TYPE OF REPORT & PERIOD COVERED Research Report; 1 February through 30 June 1974
		6. PERFORMING ORG. REPORT NUMBER
7. AUTHOR(s) Dr. Jay A. Fox Dallas N. Barr		8. CONTRACT OR GRANT NUMBER(s)
9. PERFORMING ORGANIZATION NAME AND ADDRESS US Army Mobility Equipment Research and Development Center ATTN: AMXFB-MB Fort Belvoir, Virginia 22060		10. PROGRAM ELEMENT, PROJECT, TASK AREA & WORK UNIT NUMBERS 6.11.01.A 1T161101A91A 128
11. CONTROLLING OFFICE NAME AND ADDRESS US Army Mobility Equipment Research and Development Center Fort Belvoir, Virginia 22060		12. REPORT DATE April 1975
		13. NUMBER OF PAGES 56
14. MONITORING AGENCY NAME & ADDRESS(if different from Controlling Office)		15. SECURITY CLASS. (of this report) Unclassified
		15a. DECLASSIFICATION/DOWNGRADING SCHEDULE

16. DISTRIBUTION STATEMENT (of this Report)

Approved for public release; distribution unlimited.

17. DISTRIBUTION STATEMENT (of the abstract entered in Block 20, if different from Report)

18. SUPPLEMENTARY NOTES

19. KEY WORDS (Continue on reverse side if necessary and identify by block number)

Coating removal
Laser-induced stress
Plasma trapping
Short-pulse laser

20. ABSTRACT (Continue on reverse side if necessary and identify by block number)

Results of a 4-month, experimental study of the interaction between short laser pulses and coatings of paints and water are presented. In particular, objectives of the research include: (1) A determination of the fluence levels needed to sustain damage/modification of coatings; (2) an investigation of the impulsive loading on the substrate caused by the presence of these coatings; and (3) the identification of the basic laser/coating interaction mechanism.

DD FORM 1 JAN 73 1473 EDITION OF 1 NOV 65 IS OBSOLETE

UNCLASSIFIED

SECURITY CLASSIFICATION OF THIS PAGE (When Data Entered)

SUMMARY

Camouflage coatings are designed to conceal targets in the visible and near-infrared spectral regions. If this coating were removed, the probability of being detected would be sharply increased. The research reported herein will result in a better understanding of the mechanism of paint removal by lasers and, thereby, aid in the formulation of coatings resistant to this effect.

Results of a 4-month, experimental study of the interaction between short laser pulses and coatings of paints and water are presented. In particular, objectives of the research include: (1) A determination of the fluence levels needed to sustain damage/modification of coatings; (2) an investigation of the impulsive loading on the substrate caused by the presence of these coatings; (3) the identification of the basic laser/coating interaction mechanism.

The USAMERDC 10-joule, Q-switched glass laser was used for most irradiations of the metallic targets coated with standard military paints and distilled water. Some of the more significant results are as follows:

a. Paint removal is accomplished by both direct coupling and plasma trapping, depending on the transparency of the coating to the laser radiation.

b. A few mils of paint can be removed with low fluences (< 10 J/cm^2). The amount does not appear to be a strong function of reflectivity; rather, the removal depends on both absorptivity and skin depth. Plasma-blockage effects make these low fluences more efficient in paint removal.

c. Water droplets vaporize when exposed to $\simeq 200$ J/cm^2. The average intensity at these fluences is theoretically not sufficient to cause vaporization, but the presence of hot spots in the beam can account for this.

d. The presence of the coatings can lead to spallation and/or perforation of aluminum, tin, lead, and Plexiglas substrates.

e. Rear-surface measurements of stresses generated in paint- and water-coated aluminum targets confirm the above qualitative observations. Peak stresses of more than 6 kilobars are recorded, and the stress pulse duration is increased up to a factor of three by the presence of coatings.

f. Although long pulses ($\simeq 500$ microseconds) can melt through steel, they are not as efficient as short pulses ($\simeq 30$ nanoseconds) in removing paint and in generating coating-aided stresses.

CONTENTS

ILLUSTRATIONS

ILLUSTRATIONS (cont'd)

TABLES

THE EFFECT OF SHORT-PULSE LASER RADIATION ON COATINGS

I. INTRODUCTION

1. **Objective.** The objective of this research (conducted by the US Army Mobility Equipment Research and Development Center's (USAMERDC) Countersurveillance and Topographic Division) was to investigate the effect of short-pulse laser radiation on coated metallic targets. In particular, the goals were: (a) to determine if paint could be removed by laser radiation; (b) to determine, if possible, the necessary fluence levels to do so; (c) to measure the change in impulse caused by the presence of paint and water coatings; and (d) to identify the basic mechanism by which the paint and water were removed.

II. PAINT-REMOVAL

2. **General.** A total of 12 standard military paints was used for all experiments described in this report. Figure 1 shows aluminum targets, each coated with one of the paints. Appendix A contains a description of the paints, their methods of application, their spectral properties, and the methods of thickness measurement. Appendix B gives specific information on the laser used in these experiments.

3. **Theories of Paint Removal.** Three mechanisms of paint removal were considered in this report.

a. **Vaporization.** A major purpose of this research was to identify the mechanism by which short-pulse laser radiation removes paint. Among the possibilities is direct thermal coupling in which the laser energy interacts with the target via the inverse bremsstrahlung process; heat builds up faster than the material can expand, and an explosion ensues. For conductors, the photons give up their energy to the free electrons, which can then collide with and transfer energy to the lattice phonons. Because the mean free time between collisions is on the order of 10^{-13} sec, this process can be regarded as instantaneous when compared to the duration of a typical Q-switched laser pulse ($\sim$ 30 nanoseconds). For a semiconductor, the effect is slightly modified so that the photon creates an electron/hole pair which then recombines, giving up energy to the lattice. If the main absorption of laser energy by paint occurs in the carbon-based constituents, then this semiconductor picture may be qualitatively correct. At any rate, it is important to know that, once again, the time necessary to distribute the thermal energy to the lattice is small compared to the duration of a 30-nanosecond laser pulse. Thus, local thermodynamic equilibrium is established, and the concept of temperature is valid. (Note that this may not be the case for picosecond pulses.)

Let us calculate the temperature rise T for an aluminum target exposed to a 30-nanosecond laser pulse.

From thermodynamics, the heat flow is given by:

$$\nabla^2 T(x,y,z,t) - \left(\frac{1}{\kappa}\right)\frac{\partial T}{\partial t} = -\frac{A(x,y,z,t)}{K},$$

where: T = temperature rise as a function of position (x,y,z) and time (t),

κ = thermal diffusivity,

K = thermal conductivity, and

A = heat production/volume/time.

The material considered is a semi-infinite slab with a boundary at z = 0. For a one-dimensional case, the solution for a conductor is:

$$T(z,t) = \left(\frac{2\Phi_o}{K}\right)(xt)^{1/2}\ \mathrm{ierfc}\,[z/2(\kappa t)^{1/2}] - (\Phi_o/\alpha K)\,e^{-\alpha z}$$

$$+ (\Phi_o/2\alpha K)\exp(\alpha^2\kappa t - \alpha z)\ \mathrm{erfc}\,[\alpha(\kappa t)^{1/2} - z/2(\kappa t)^{1/2}]$$

$$+ (\Phi_o/2\alpha K)\exp(\alpha^2\kappa t + \alpha z)\ \mathrm{erfc}\,[\alpha(\kappa t)^{1/2} + z/2(\kappa t)^{1/2}],$$

where: erfc = complementary error function,

ierfc = the integral of erfc,

α = absorption coefficient, and

Φ_o = absorbed power density.[1]

Instead of evaluating this cumbersome form, we may simplify in the following manner. If we are dealing with a conductor, $\alpha \approx 10^5$ to 10^6 centimeters,$^{-1}$ and if the laser pulse is constant in time and uniform in spatial extent,

$$T(z,t) = \frac{2\Phi_o(\kappa t)^{1/2}}{K}\ \mathrm{ierfc}\,(z/2(\kappa t)^{1/2}).$$

At the surface,

$$T(0,t) = \frac{2\Phi}{K}\left(\frac{\kappa t}{\pi}\right).$$

---

[1] H.S. Carslaw and J.C. Jaeger, *Conduction of Heat in Solids*, 2nd Ed., Chapter 2, Oxford Univ. Press, London and New York, 1959.

Figure 1. Paint samples used in the experiments. All of the colors are reproduced fairly well with the exception of red and fluorescent orange, both of which appear considerably brighter to the eye.

For aluminum, if the target absorbs the rather low fluence (energy density) of 0.7 J/cm^2 in 30 nanoseconds, the temperature increase is:

$$T(0,t) = 1{,}820^\circ\ C,$$

which is enough to vaporize the surface.

Although the preceding exercise contained simplifying assumptions, it nevertheless correctly predicts the order of magnitude of fluence necessary to vaporize aluminum. Furthermore, although the calculation strictly holds only for a conductor, experimental results show that the order of magnitude of temperature increase is also correct for paints (one also can show this mathematically). Thus, the fluences used for these experiments are capable of vaporizing both the paint and the substrate on which it is deposited.

When the material is vaporized, the blowoff rapidly expands (10^6 to 10^7 cm/s), absorbs the rest of the incoming laser energy (assuming that all the pulse was not needed to cause vaporization), and becomes thermally ionized (10^4 to $10^5\,^\circ$ K), thus creating a plasma. At some critical density, the plasma will become opaque to the laser energy and will shield the surface. It is then possible that this plasma itself will reradiate energy at a later time and that this energy can reach the surface. (We have obtained experimental evidence of this reradiation phenomenon, which is discussed in paragraph 4a.)

These short-pulse lasers do not evaporate large amounts of material. The laser energy does not go into supplying the latent heat of vaporization but instead goes into raising the temperature of the small amount of material evaporated in the beginning of the pulse. Therefore, although we have shown that direct thermal coupling is likely to produce vaporization of a painted surface, it is not at all obvious that this mechanism can itself supply enough energy to vaporize a significant thickness of paint before the self-shielding phenomenon initiates.

b. **Shock.** At the beginning of this research there appeared another possible candidate for the mechanism at least partially responsible for paint removal. When the energy is coupled into the paint, a compressive stress wave propagates into the target. For a 1-D elastic wave, the stress σ is related to the strain ϵ in the material by:

$$\sigma = \frac{1 - \nu}{(1 + \nu)(1 - 2\nu)} E\,\epsilon,$$

where:

ν = Poisson's ratio, and

E = Young's modulus.

At the paint-substrate boundary, part of the stress σ_t is transmitted and part σ_r is reflected (both compressive):

$$\sigma_t = \sigma \frac{2\rho_2 \, U_{s_2}}{\rho_2 \, U_{s_2} + \rho_1 \, U_{s_1}} \text{, and}$$

$$\sigma_r = \sigma \frac{\rho_2 \, U_{s_2} - \rho_1 \, U_{s_1}}{\rho_2 \, U_{s_2} + \rho_1 \, U_{s_1}} \text{,}$$

where:

ρ_1, ρ_2 = densities of paint and substrate, respectively, and

U_{s_1}, U_{s_2} = shock velocities in paint and substrate, respectively.

As can be seen, most of the stress wave is transmitted into the substrate where it will encounter the free surface at the rear and reflect in tension. When this tensile pulse arrives at the paint-substrate interface, debonding may occur since tensile stresses of several thousand atmospheres can be produced easily with short laser pulses. (We have verified these speculations with the aid of calculations made with the PISCES Lagrangian hydrodynamic code.)

c. **Plasma Trapping.** It became evident that the appearance of the irradiated targets fell into two categories as the photographs in Figure 2 will show. Both samples have been coated with about 1.0 mil of paint; the top sample was irraditated with four shots of 1.3 J/cm^2 each, while the bottom was irradiated with one 1.3-J/cm^2 shot. As shown in Figure 2, the olive drab (OD) paint gives the visual appearance of having been burned off, while the red paint appears to have been blasted off as if there had been an explosion under the surface. Note also that the aluminum substrate is relatively unmarked in the OD case as compared to the red case. This "blasted" appearance was noted in several of the paints, namely white, both types of orange, lusterless olive drab, field drab, and forest green.

The following theory was developed to explain this appearance. If the paint were at least partially transparent to 1.06-micrometer radiation, then part of the energy should be transferred to the substrate. Even if a small percentage of this energy

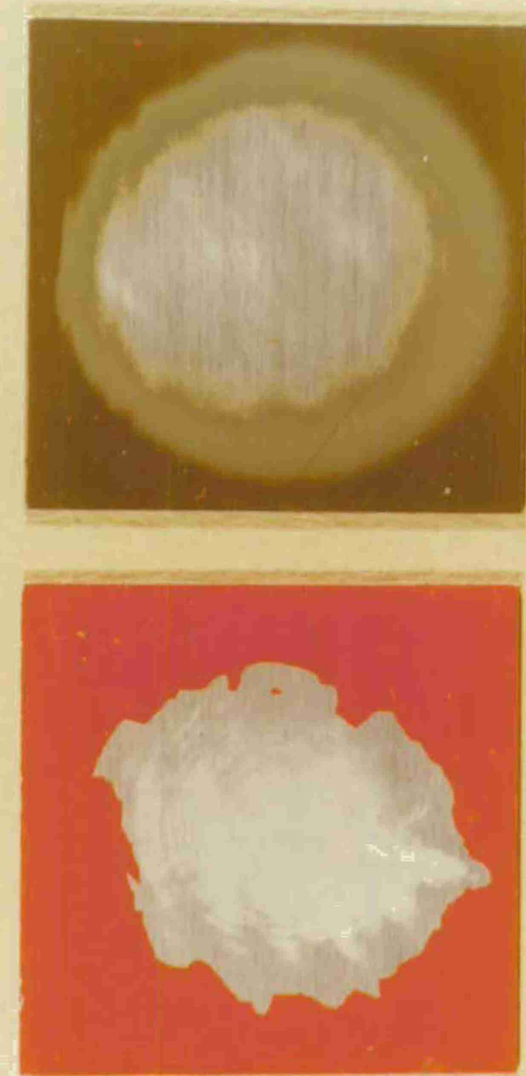

Figure 2. Samples of approximately equal paint thickness, showing two basic mechanisms by which paint may be removed. Top (olive drab): direct coupling. Bottom (red): plasma trapping.

couples into the metal, vaporization can occur. As the temperature rises, the plasma tries to escape but is momentarily confined by the paint. The pressure builds up until an explosion ruptures the paint layer and releases the trapped gas. This would account for the appearance both of the paint and of the substrate.

4. Measurement of Paint Removal.

a. **Vaporization.** The amount of paint removed was measured with an Ainsworth Type 24N analytical balance which could be read directly to 10 micrograms. Repeated measurements of the same sample yielded results consistent to within ± 5 percent.

A quantitative idea of how much fluence can remove a certain amount of paint can be obtained from Figure 3. It can be seen that 1 microgram of black paint can be removed by 300 J/cm^2. This graph is somewhat deceptive, however, in that it does not point out the fact that even the lowest fluence (30 J/cm^2) was capable of removing enough paint to uncover the substrate (the paint thickness was 0.5 mil). Although the laser beam was focused to the same spot diameter for each fluence, the diameter of the exposed substrate was smaller for lesser fluences. This is at least partially because of the gaussian energy distribution of the beam.

At these high fluences, the amount of mass removed was not a strong function of the paint reflectivity as Table 1 shows.

Table 1. Effect of Reflectivity on Mass Removed

Color	Mass Removed (Mg)	Reflectivity (Pct) @ 1.06 μm
White	0.070 ± 0.011	80
Blue	0.153 ± 0.004	21
Black	0.103 ± 0.003	3

The total fluence in each case was about 300 J/cm^2; the indicated error represents the average deviation calculated from 10 irradiations. The anomalous behavior of these results initially was believed to be at least partially caused by the well-known phenomenon that materials subjected to intense, short-pulse laser radiation exhibit reduced reflectivity. Section 4c will show that the actual major cause is probably plasma trapping.

An attempt was made to investigate whether or not paint removal was cumulative. That is, do two irradiations at half a certain energy remove as much as one shot at the full energy? Many measurements were taken, but the results may be expressed best by the following, which is based on black paint.

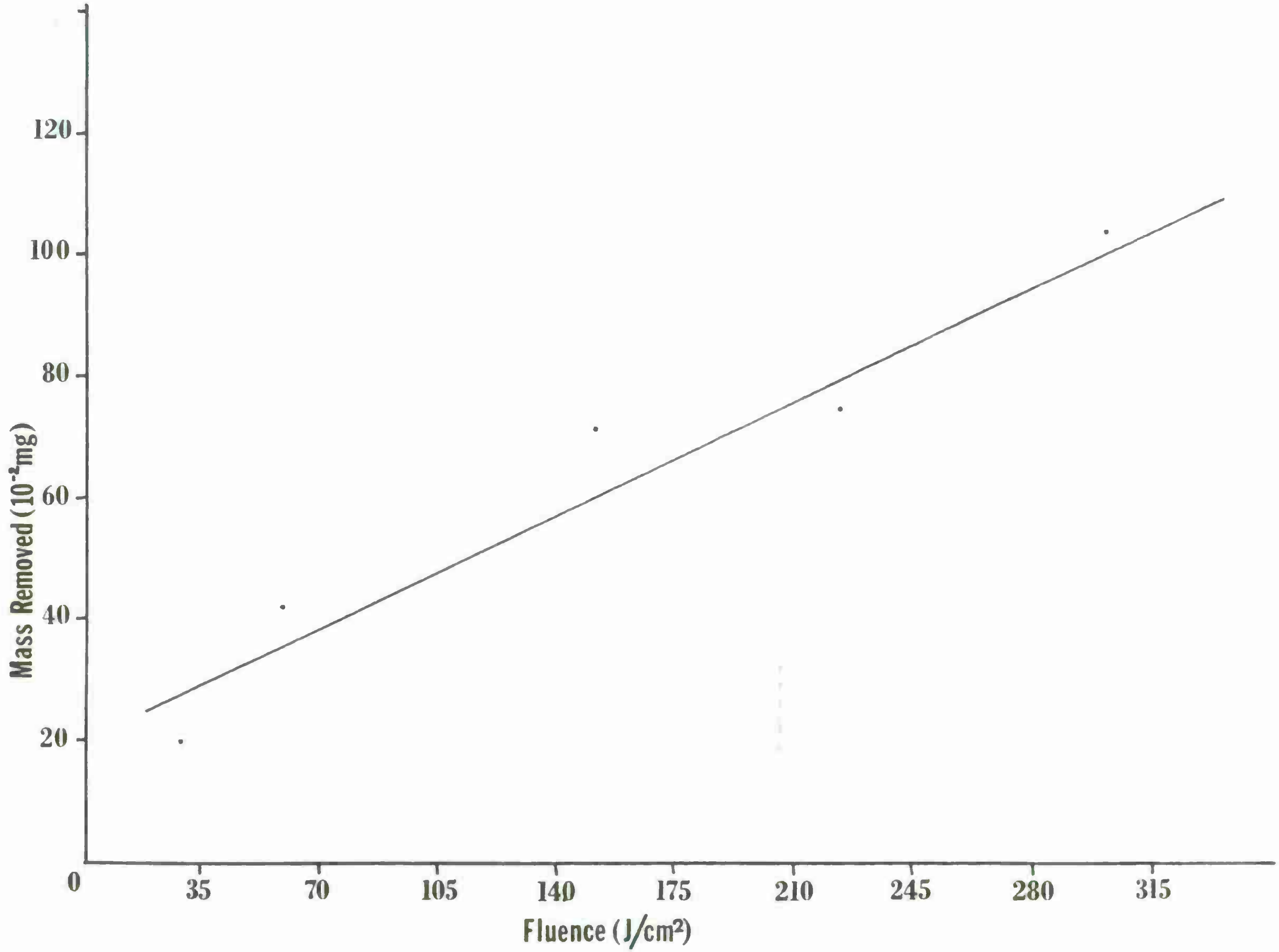

Figure 3. Mass of paint removed from a black target as a function of fluence.

Number of Shots Times Relative Energy = Total Energy (Arbitrary Units)	Paint Removed Down to Substrate?
1 x 1 = 1	No
2 x 0.5 = 1	Yes
1 x 0.5 = 0.5	No
5 x 0.1 = 0.5	Yes
10 x 0.05 = 0.5	Yes

The paint thickness in this case was 1.1 mil. Obviously, the removal was even better than cumulative! That is, it is apparent that *more* mass is being removed by many separate shots at low fluence than by an equivalent single shot of high fluence.

This is not the result of the first shot preparing the surface of the target so that the succeeding shots couple in more efficiently. Measurements have shown that the amount of mass removed by the first shot is virtually equal to that removed by any of the following shots. The phenomenon also is not dependent on the color paint used; all paints exhibited this behavior. Figure 4 shows the results of a typical set of shots.

The target on the left has been irradiated with a single shot of 150 J/cm^2, the middle one was impacted with two shots of 75 J/cm^2 each, and the target on the right was irradiated with 10 shots of 15 J/cm^2 each. Note that the paint has been entirely removed in the irradiated regions of the middle and right-hand targets; the aluminum substrate is clearly visible. All beam diameters were the same; the apparent difference in the removed areas is caused by the spatial gaussian variation in the laser beam.

The fact that lower fluence shots were more efficient in removing mass than the more energetic pulses suggested that the hotter and denser plasmas formed by the higher energy shots were blocking the target from the rest of the laser pulse. As the reader will recall, we had speculated as to the shielding of a target because of blowoff. We had further indicated the possibility of reradiation of the blowoff itself. Such behavior was in fact observed in the following experiment.

A painted target was illuminated with a fluence of approximately 300 J/cm^2. A photodiode was used to record the emission from the plasma generated at the front surface of the sample. Figure 5 is a typical oscilloscope record of such a shot. Note first that the plasma radiation lasted for about 800 nanoseconds, which is much longer than the duration of the laser pulse itself ($\simeq$ 20 nanoseconds). Then, note the presence of a secondary peak starting about 100 nanoseconds after the beginning of the pulse. It is this secondary maximum that is the manifestation of the reradiation phenomenon. This feature should be a strong function of fluence because it depends on how much laser energy was absorbed by the plasma. The following set of data illustrates

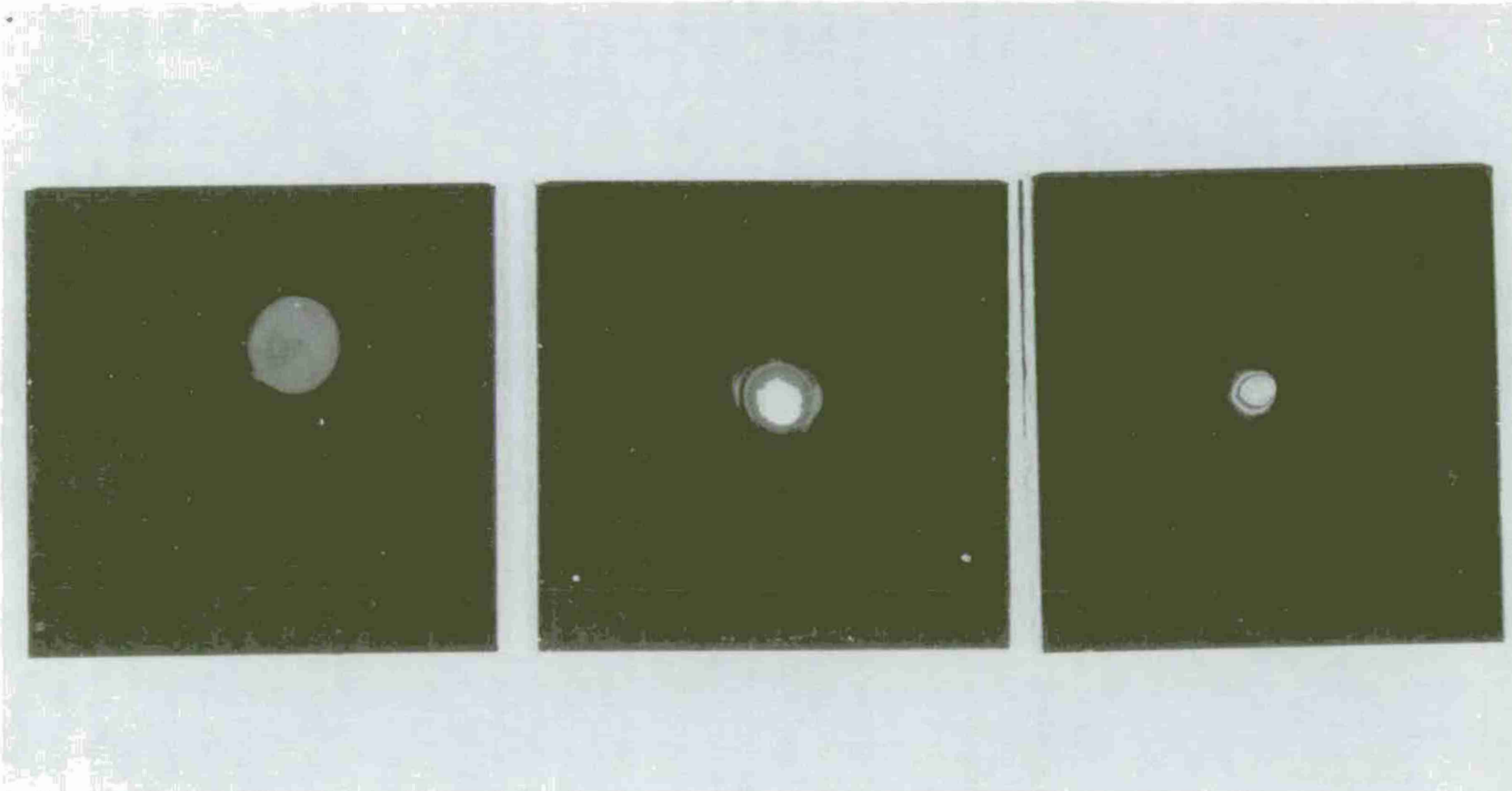

Figure 4. The cumulative effect of short laser pulses on paint. The total fluence on each target is the same, but the number of shots is (from left to right) one, two, and ten.

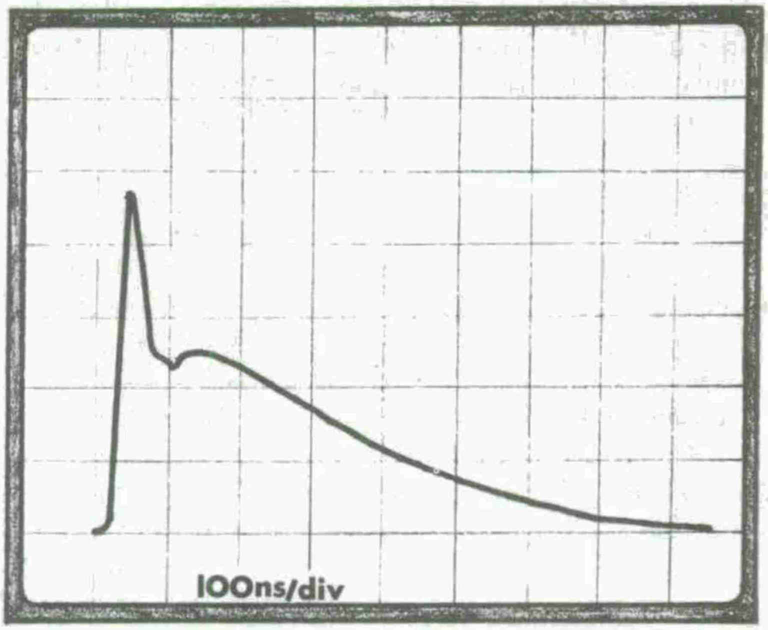

Figure 5. A typical oscilloscope trace of the light emitted by the plasma of a target irradiated with short laser pulses, as recorded by a photodiode.

that this is indeed the case:

Relative Height of Secondary Peak Compared to Primary	Relative Fluence
0.54	1
0.45	0.5
0.14	0.2
0.00	0.1

Since the presence of this secondary peak indicates that energy is being "wasted" in the plasma instead of being coupled into the paint, less fluence may be more efficient in removing mass than more fluence.

This is indeed the case as an examination of Figure 6 will show.

The single shot at high fluence did not remove all the paint, while three shots at 300 J/cm^2 and three shots at 1 J/cm^2 exposed the aluminum substrate. Thus, it is clearly much more efficient to remove paint with low-fluence shots than with high-fluence ones. Measurements show that from the point of view of energy low-fluence shots are 200- to 300-times more efficient, while from cleared-area considerations they are 8- to 10-times as efficient. It should be noted that all types of paint tested exhibited this same behavior (i.e., more paint could be removed with a lesser fluence). The method of sample preparation also does not affect the results. In addition to targets which had been spray painted and brush painted, samples were selected where the paint had been applied over an undercoat and then baked. The phenomenon in question was still observed.

b. **Shock.** In addition to paint removal by vaporization, it was suggested that the laser-induced stress wave would, after reflection from the rear surface of the target, cause debonding by means of the tensile pulse interacting at the paint/metal interface. Since the forces are likely to be quite large (i.e., 1 kilobar, or 1,000 x 15 lbf/in^2), the paint could be ejected at great velocities, thus giving rise to another stress wave. Note that this wave would arrive at the rear surface at a much later time than would the one caused by a direct coupling mechanism. Thus, two stress waves, one caused by the initial coupling and the other caused by the paint blowoff, would be recorded by a gage mounted on the rear target surface. This experiment has been performed and is described in detail in Section III. The results show that the second pulse is not present.

The recorded shape of the stress waves was essentially the same at long times for painted and unpainted targets. The initiation of the stress occurred at the same time for both types of targets. For example, during one set of tests it was found that the stress wave began at 142.8 ± 0.6 nanoseconds when a base aluminum target was irradiated and at 142.1 ± 1.0 nanoseconds when a black painted target was used. The time was measured by triggering the oscilloscope externally, and the indicated error is the average deviation from sets of 10 measurements. Thus, it does not seem likely that the reflected stress wave participates in the paint-removal process.

c. **Plasma Trapping.** In order to test this theory, orange paint was sprayed onto the surface of both Plexigas and aluminum. Radiation of the 1.06-micrometer wavelength passes through clear Plexiglas with almost no attenuation, and such radiation definitely does not generate a plasma on the surface when it is impacted with light of this wavelength. Thus, if the above hypothesis were correct, there should be more orange paint removed from the aluminum than from the Plexiglas (i.e., there will be no plasma to trap with the Plexiglas). The results of this test gave values of mass removal of $(49 \pm 5) \times 10^{-2}$ milligrams for Plexiglas and $(900 \pm 70) \times 10^{-2}$ milligrams for aluminum. Thus, almost 20 times as much mass was removed using the aluminum substrate. Paints that did not exhibit this "blasted-off" appearance were also tested and did not indicate similar dependence on the substrate. Other "blastoff" paints give similar results to the orange.

However satisfactory the above experiment might seem in demonstrating that the plasma confinement theory is valid, more direct evidence would be even more convincing. To that end, the reflection (and, indirectly, the transmission) of the paint

Figure 6. Field drab sample irradiated with one and three high-fluence (300 J/cm^2) shots (upper left and right, respectively) and three low-fluence (1 J/cm^2) shots (middle).

was measured using the spectrophotometer described in Appendix A. A qualitative idea of whether or not the paints were transparent was obtained by rating the dependence of measured reflectance on paint thickness. If the paint were transparent at a given wavelength, the spectrophotometer would "see" light being reflected from the substrate as well as from the paint surface. Because aluminum had a reflectance at 1.06 micrometers–not much different than many of the paints (~ 62 percent) – a lead substrate (reflectance of ~ 20 percent) was used for many of these tests. A few results are given in Table 2.

Table 2. Paint Reflectance

No. of Coats	Color	Reflectance at 1.06 μm (Pct)
1	Fluorescent	25.0
2	Orange	34.5
3		51.0
1		62.5
2	White	75.5
3		80.0
1		3.0
2	Black	3.0
3		3.0
1		21.0
2	Blue	21.0
3		21.0

Thus, it is proven that the paints with the "blasted-off" appearance are those which are at least partially transparent to 1.06-micrometer radiation, and the plasma-trapping hypothesis has been demonstrated to be valid. Another more accurate method of measuring transmission of these paints is described in Appendix A.

III. LASER-INDUCED STRESS IN COATED TARGETS

5. **Damage Enhancement.** It has been discovered in the Countersurveillance and Topographic Division laboratory and in others that coating a target with water increases the impulse transmitted to the target; hence, damage to the target is also increased.[2] [3]

[2] J.A. Fox, Appl. Phys. Lett. *24*, 461 (1974).

[3] M. Siegrist and F. Kneubuhl, Appl. Phys. 2, 43 (1973).

Both of these phenomena will be discussed in this section and in section 6.

The mechanism for this increased impulse has been suggested to be the following: The water absorbs enough of the radiation to vaporize. The resulting explosion produces a reaction that drives a compressive wave into the target. Since the mass of water ejected is much larger than the typical blowoff from an uncoated target, one could expect the resulting stress to be greater also (assuming the ejected velocities were not too dissimilar). Let us calculate the amount of laser fluence necessary to produce this vaporization.

The amount of energy absorbed U by a water layer of thickness z and absorptivity α can be expressed as:

$$U_a = U_{inc} - U_{inc}\, e^{-2\alpha z},$$

where U_{inc} = the energy actually entering the water layer at z = 0. (See Appendix C.)
Also, $U_a = mc_p \,\Delta T$,

where: m = mass of water,
c_p = specific heat, and
ΔT = temperature increase.

Combining the equations gives:

$$\Delta T = \frac{U_{inc}\,(1 - e^{-2\alpha z})}{mc_p} \; .$$

This may be expanded and expressed in terms of the density ρ and area A of the water layer:

$$T = \frac{U_{inc}\left(1 + 2\alpha z - \left(\frac{2\alpha z}{2}\right)^2 + \ldots\right)}{\rho\, Az\, c_p} \; .$$

For a typical water drop, we use as the layer in question

$\alpha = 0.0166$ millimeter^{-1}, and

$z \approx 2$ millimeters.

Thus, we are justified in expressing the temperature increase as:

$$\Delta T = \frac{2\alpha\, U_{inc}}{\rho\, A\, c_p} \; .$$

But $\frac{U_{inc}}{A}$ is the fluence F by definition.

Thus, $\Delta T = \frac{2\alpha F}{\rho c_p}$.

Inserting the numerical values for water and expressing the fluence in joules per square centimeter, we get:

$$\Delta T\ (^\circ C) = 7.92 \times 10^{-2}\ F.$$

Assume that 200 J/cm^2 is incident on the water drop and that this fluence is entirely absorbed. Then, $\Delta T = 16^\circ$ C.

In other words, no vaporization should occur. However, it appeared to us that such fluences *did* vaporize a drop on the surface of a target. Since it was possible that the target surface itself was causing the vaporization, the experiment sketched in Figure 7 was devised.

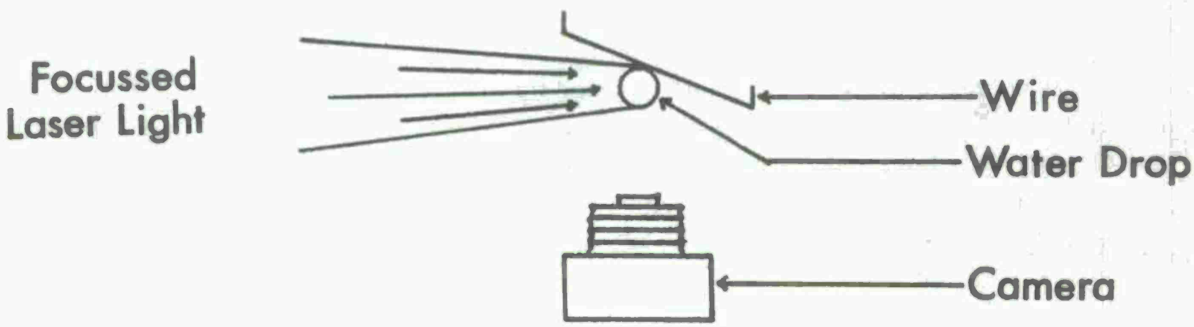

Figure 7. Water-drop experiment.

As shown in the figure, a water drop (~ 2 millimeters in diameter) was suspended from a thin wire. The laser radiation was focused so that a fluence of about 200 J/cm^2 was incident on the drop. An aperture was used to prevent the radiation from impacting the wire, and the event was recorded by means of a camera and 3,000-speed, Polaroid film. Clear evidence of water vaporization was observed. Timing data were gathered from monitoring the broad spectral emission from the water target. The results suggest that the explosion occurs about 10 nanoseconds after impact, i.e., almost at the peak of the 24-nanosecond pulse. Thus, even though a calculation shows that no vaporization should occur, obviously it does.

Others also have noted that vaporization occurs at much lower fluences than were thought to be possible.[4] A theoretical explanation has been derived and is based on the fact that the typical Nd/glass laser emits multi mode radiation with many "hot spots" in the beam that may have up to 50 times the peak intensity derived by dividing the total energy by the pulse duration.[5] [6] This theory is based on certain thermodynamic arguments used in conjunction with the Rayleigh and heat-conduction equations. Since the results take into account the actual absorption of water at 1.06 micrometers and accurately predict both the time of explosion and the velocity of the ejecta, this explanation seems quite sound. At any rate, there is no doubt that vaporization occurs and that the reaction to this causes a strong impulse to be generated.

However, another mechanism also is at work here. It will be shown in paragraph 6b that the impulse delivered to a target increases *even when fluence is insufficient to cause water vaporization.* For example, the unfocused laser beam (~ 1 J/cm^2) will not cause vaporization of a drop held suspended from a wire as was described earlier, and yet a target will receive more impulse when coated with a similar drop and irradiated with 1 J/cm^2.

We have conducted experiments that give an explanation for this phenomenon. Fluences as low as 0.1 J/cm^2 can cause vaporization in solid targets irradiated with a Q-switched laser pulse. According to both our measurements and others, only 6.4 percent of the 1.06-micrometer light gets absorbed in the water drop at low fluences.[7] This means that almost all of a 1-J/cm^2 pulse can cause vaporization of the surface under the drop; the drop then traps the plasma until high stresses are built up, thus shattering the drop and giving rise to increased stresses on the substrate. Therefore, once again, as in the case of partially transparent paints, both direct absorption and plasma trapping act to increase stress levels.

As implied in the previous paragraphs, the increased stress levels caused by either or both the paint or the water coating shattering and being ejected from the surface of the target at high velocity can cause increased damage to the target. We have, in fact, observed such damage.

Figure 8 shows the front view and Figure 9 shows the back view of 0.2-millimeter thick, 1100-aluminum targets. The target on the left was uncoated, the middle one had a water coating, and the one on the right was coated with both olive

---

[4] V. V. Burinov and S. A. Sorokin, Sov. J. Quant. Electron. *3*, 89 (1973).

[5] *Ibid.*

[6] T. M. Barkhudarova *et al.*, Sov. Phys. JETP *22*, 269 (1966).

[7] Burinov and Sorokin, *op. cit.*

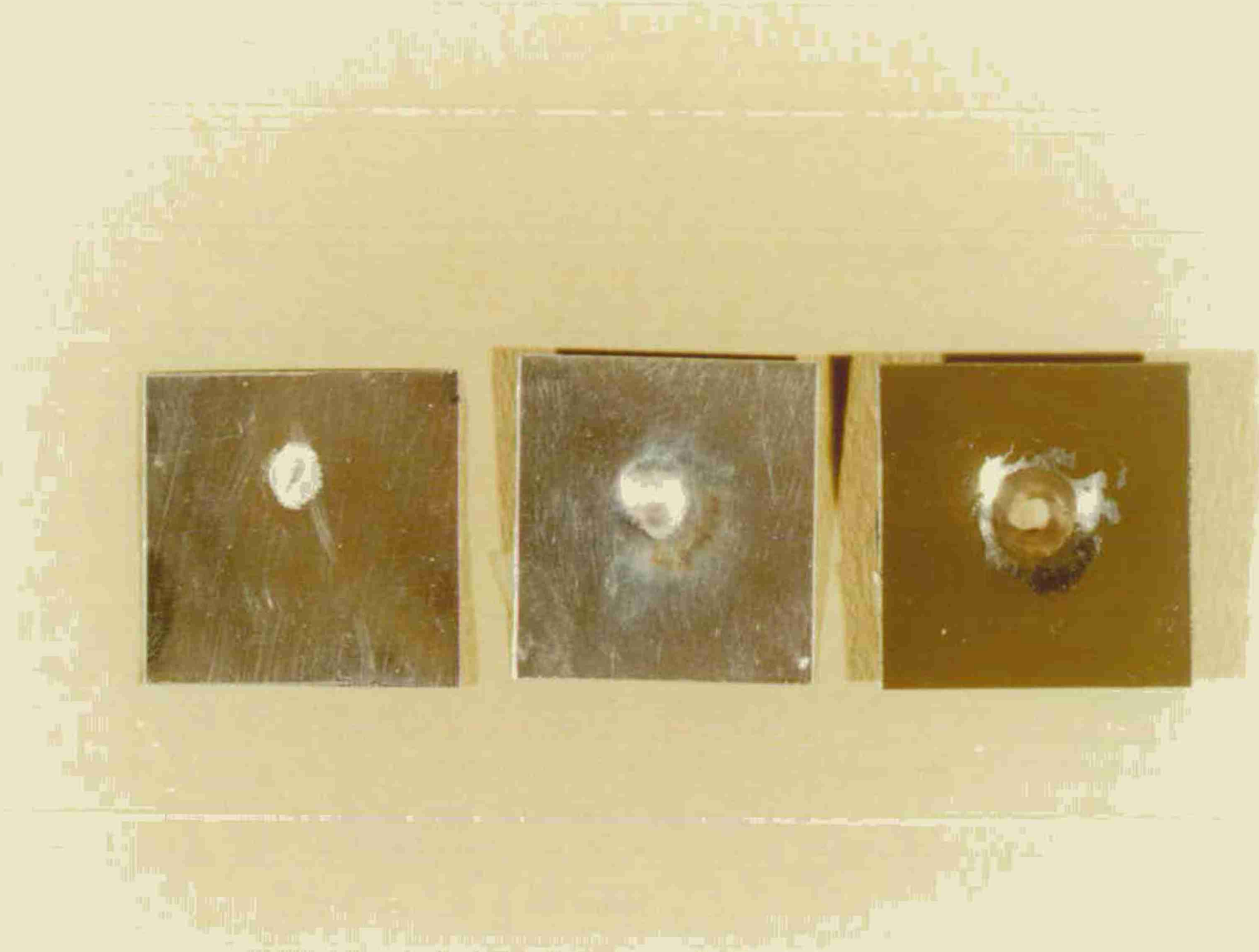

Figure 8. Front view of thin, aluminum targets irradiated with a 200-J/cm^2 fluence. (Left – uncoated; center – water coated; right – paint and water coated.)

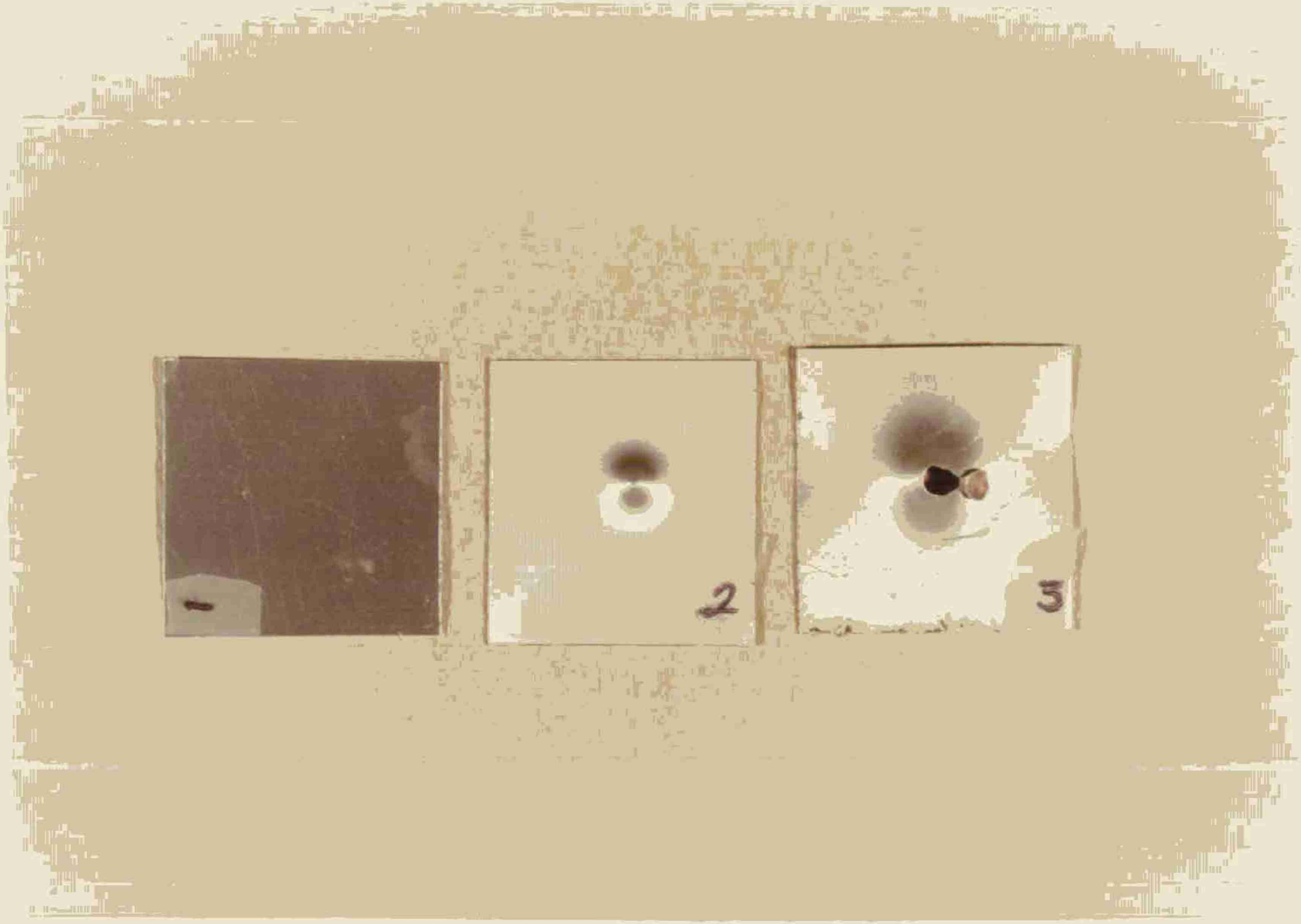

Figure 9. Rear view of thin, aluminum targets irradiated with a 200-J/cm^2 fluence. (1 – uncoated; 2 – water coated; 3 – paint and water coated.)

drab paint and water. The fluences on target were 200 J/cm^2. The front surface of the uncoated target was vaporized to a depth of a few micrometers and no damage was observed at the rear face. The water-coated target was almost perforated, the depth of the crater being at least 2 millimeters. The target coated with both the paint and the water was perforated (diameter $\approx$ 4 millimeters), and it failed in the so-called plugging mode. (According to one group, this is the result of late time deformation caused by the interaction of transverse elastic-plastic stresses.[8]) Another, more quantitative idea of the comparative damage done by water and paint coatings may be obtained from the fact that the perforation threshold for just the water coating is 310 J/cm^2 (i.e., more than 50-percent greater than the combination). This agrees with the stress-wave measurements presented in paragraph 6.

Not only perforation, but backface spallation has been achieved in samples of lead, aluminum, tin, and Plexiglas. It was not necessary to coat any of these targets with paint in order to achieve the spallation, but the paint enhanced the effect. Figure 10 shows a view of sectioned samples of 0.50-millimeter-thick aluminum. Neither sample had a coating of paint but had only a water drop about 2 millimeters in diameter on the surface. Since the beam was focused to such a small diameter, precise fluence measurements were not possible, but the range is 200 to 400 J/cm^2. Note that there is internal as well as complete spallation.

Spallation in Plexiglas was achieved with fluences of less than 200 J/cm^2 and just a water coating. Spallation was observed in samples as thick as ½ inch. The fact that clear Plexiglas is transparent to 1.06-micrometer radiation gives additional proof that for high fluences the water blowoff is caused by direct vaporization of the drop and not by plasma confinement. (No plasma can be formed at the surface of Plexiglas.)

Finally, some preliminary data on the effect of paint thickness were obtained. Figure 11 shows the effect of irradiating a 0.8-millimeter-thick lead target coated with white paint and a water drop; the fluence levels were about 200 J/cm^2. The thickness of each coat was about 0.8 mil (0.02 millimeter). Apparently, increasing the paint thickness moves the spall plane closer to the rear face of the target while it increases the lateral extent of the spall plane. These phenomena are not yet well understood, and we would like to defer judgment until the relevant code calculations can be made.

6. **Instrumented Stress Measurements.** In order to quantify these results and eventually understand them sufficiently to develop a predictive model, stress gage measurements were taken. Aluminum targets (1-millimeter thick) of the 6061-T6 alloy were used and the magnitude of the stress developed was measured with a quartz stress gage which was coupled to the target by a thin layer of mineral oil as has been described

[8] J. D. O'Keefe *et al.*, J. Appl. Phys. *44*, 4622 (1973).

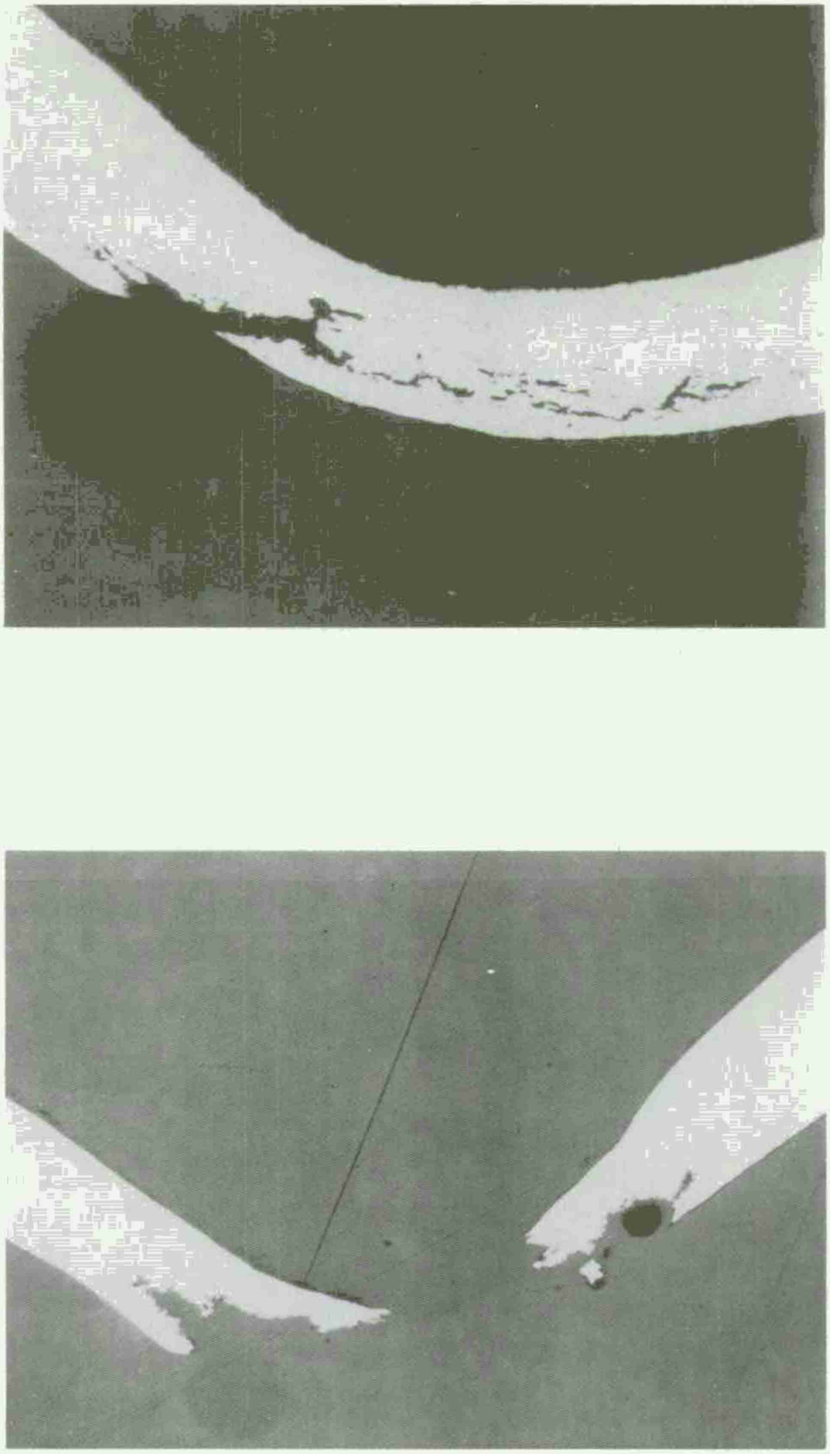

Figure 10. Aluminum samples coated with water and olive drab paint, showing both internal and complete perforation. In both instances, the laser pulse was incident from the top.

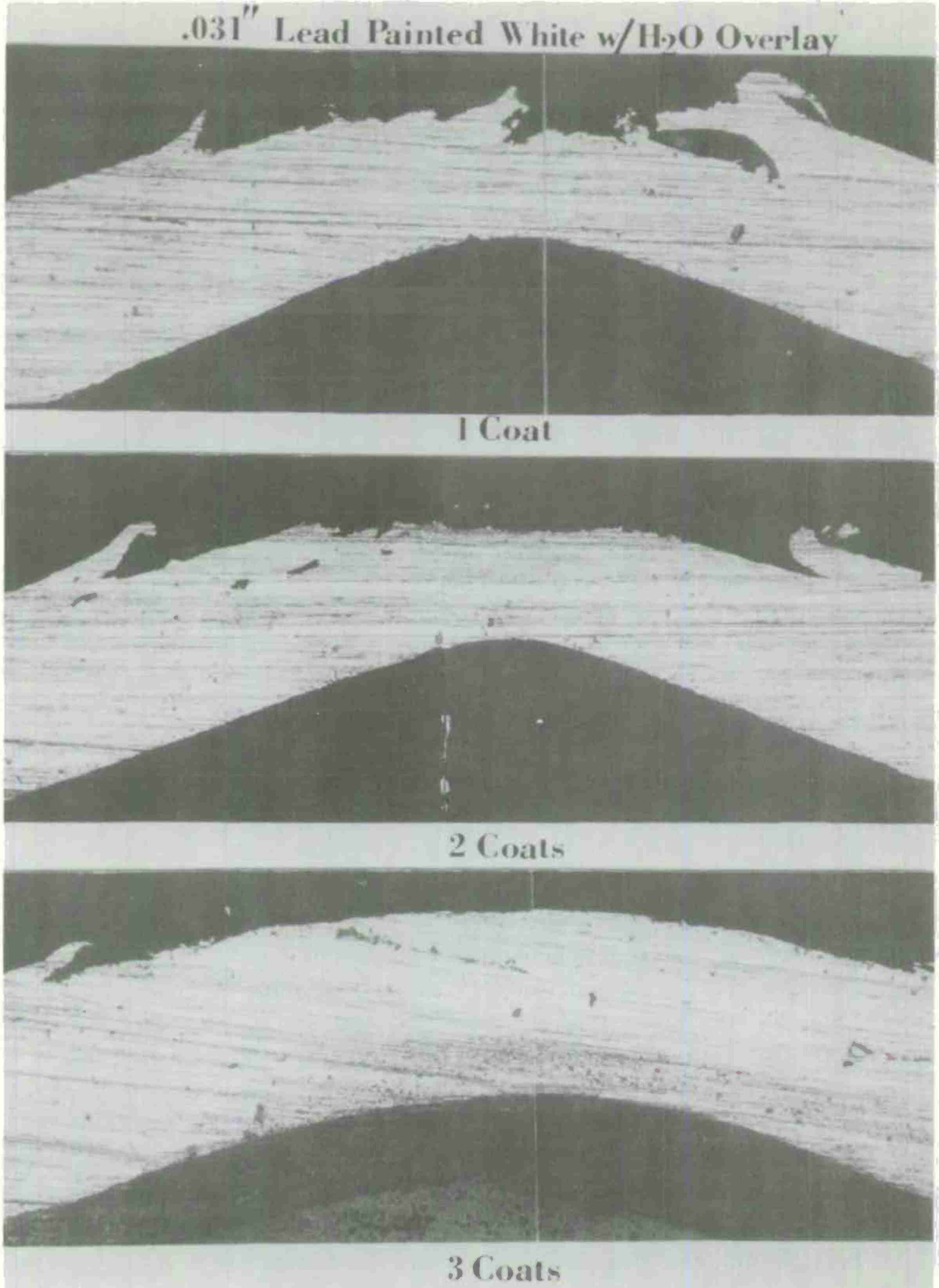

Figure 11. Cross-section of three lead targets painted white and coated with a film of water. The laser pulse was incident from the bottom.

previously in the literature.[9] In order that the gage respond to an essentially uniaxial stress, the diameter of the laser beam was larger than the diameter of the gage (0.28 centimeter) and was three times the thickness of the target. The thickness of the gages was 0.25 millimeter, which corresponded to an acoustic transit time of about 110 nanoseconds, a sufficiently long writing time to allow most of the stress wave to be recorded. Target coatings were provided by either a small drop of distilled water (2 to 4 millimeters in diameter), a thin coat of spray paint, or a combination of the two.

A clear illustration of the effect of the coatings may be seen in Figure 12, which shows the temporal history of four stress waves recorded by the quartz gages affixed to the backface of the aluminum targets. Target (1) was uncoated and was irradiated with 30 J/cm^2, target (2) was painted, target (3) was water coated, and target (4) was both painted and water coated. The fluence incident on targets (2), (3), and (4) was about 10 J/cm^2. The main effect of the paint is to increase the peak stress. The half-width of the stress wave is not significantly different from either that of the wave recorded at the rear of the uncoated sample or that of the laser pulse itself (i.e., about 30 nanoseconds). On the other hand, not only does the water coating increase the peak stress, but also the pulse width has now doubled to about 60 nanoseconds. Finally, a combination of the paint and water coatings provides yet another increase in peak stress and pulse width. Thus, the total impulse transmitted to a sample should be considerably increased by the presence of these coatings; indeed, we have presented qualitative evidence of this in the preceding portion of this report. At the present time, we have measured peak stresses as large as 3.9, 5.3, and 6.4 kilobars on painted, water-coated, and water-plus-paint-coated surfaces, respectively. In all cases, the incident fluence was about 25 J/cm^2. The effect of many high-fluence shots could not be investigated with the comparatively low-energy ($<$ 10-joule) laser utilized for all the previously mentioned experiments. The laser spot diameter would have to be decreased to such an extent that a one-dimensional stress wave would not be recorded at the backface of the target. Thus, the Battelle laser (Battelle Columbus Laboratories, Columbus, Ohio) was used to provide this extension of the investigation. This laser can provide a 140-joule pulse in 1.5 nanoseconds. No stress measurements were obtained with paint coatings; but it was found that when a water-coated sample was irradiated with a 1.5-nanosecond pulse of 170 J/cm^2, a stress of about 10.5 kilobars was recorded at the backface. The leading edge of this pulse was not as steep-fronted as those observed for stress levels below about 6.5 kilobars but, instead, was split into regions of different slopes. This suggests that the elastic limit was exceeded and that the elastic precursor was followed by a plastic loading wave. We have performed a calculation using the PISCES 1-DL, finite-difference, Lagrangian code, which shows that such a wave magnitude and shape is possible if the front surface has been impacted with a pressure of about 42 kilobars. For the purpose of this calculation, the front-surface stress wave was

[9] J. A. Fox and D. N. Barr, Appl. Opt. *12*, 2547 (1973).

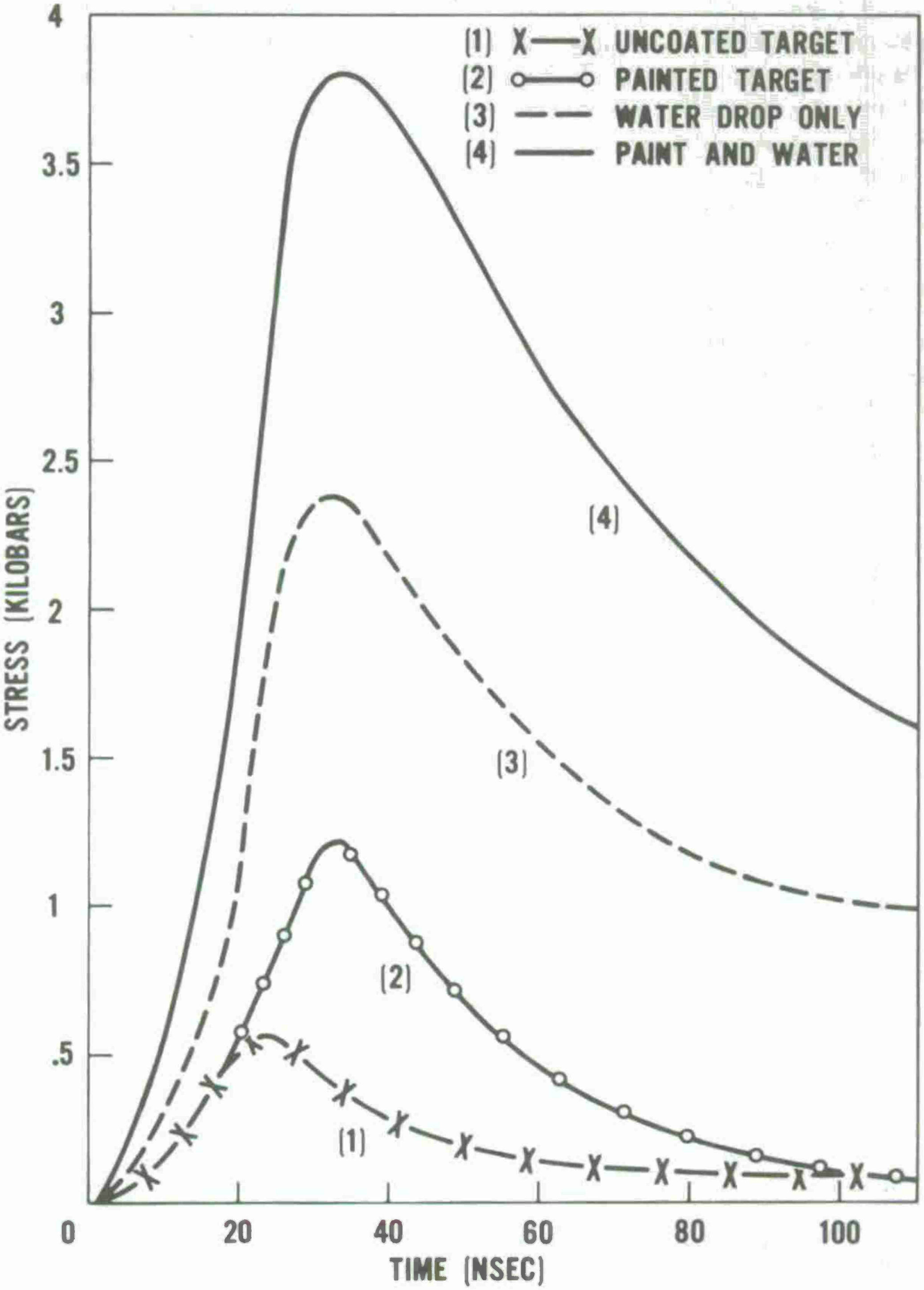

Figure 12. Temporal history of stress waves recorded at the rear face of 1-millimeter-thick aluminum targets for various coatings.

assumed to have a half-width of 12 nanoseconds, which was the minimum observed when an uncoated target was irradiated with small fluences. (Recall that we are now describing experiments performed with a 1.5-nanosecond laser pulse.) The calculated half-width at the rear surface was 38 nanoseconds, while the measured value was 48 nanoseconds. This discrepancy is at least partially because of the above assumption, i.e., that the initial half-width is as small as 12 nanoseconds. Because of the water coating, the half-width is almost surely greater than this; but this information is not presently available.

Figures 13 and 14 show the difference between the stresses generated by various fluences for uncoated and painted (black) targets. At these low fluences, the presence of the paint increases the peak stress by a factor of almost 10. Note, however, that as the fluence increases, the stress generated by the painted target is leveling off. Once again, we have evidence that high fluences tend to produce a self-shielding effect in painted targets.

a. **The Effect of Different Colors on Stress-Wave Formation.** Some preliminary data were gathered concerning the effect of different paint colors on stress production. The aim of this research is to tie these data in with the mass-removal experiments in order to eventually develop a predictive mass-removal model. Insufficient data have thus far been gathered, but a few of these will be presented as examples in Table 3.

Table 3. Stress-Wave Data for Painted Targets

Color	Thickness (Mils)	Stress Peak (Arbitrary Units)	Width of Stress Wave of Half-Maximum (Nsec)
Bare Al	NA	35	27
Black	0.7	350	24
Black	1.3	520	23
Black	2.1	660	24
OD	0.7	620	27
OD	1.3	785	29
OD	2.0	820	27
White	0.9	255	32
White	1.1	275	38
White	1.7	182	40
White	2.3	132	56

From these and other tests, the following observations have been made.

(1) The peak stresses for OD-coated targets are greater than for black-coated ones. This follows the trend indicated by the mass-removal experiments where it was measured that more mass is removed from OD surfaces than from black surfaces.

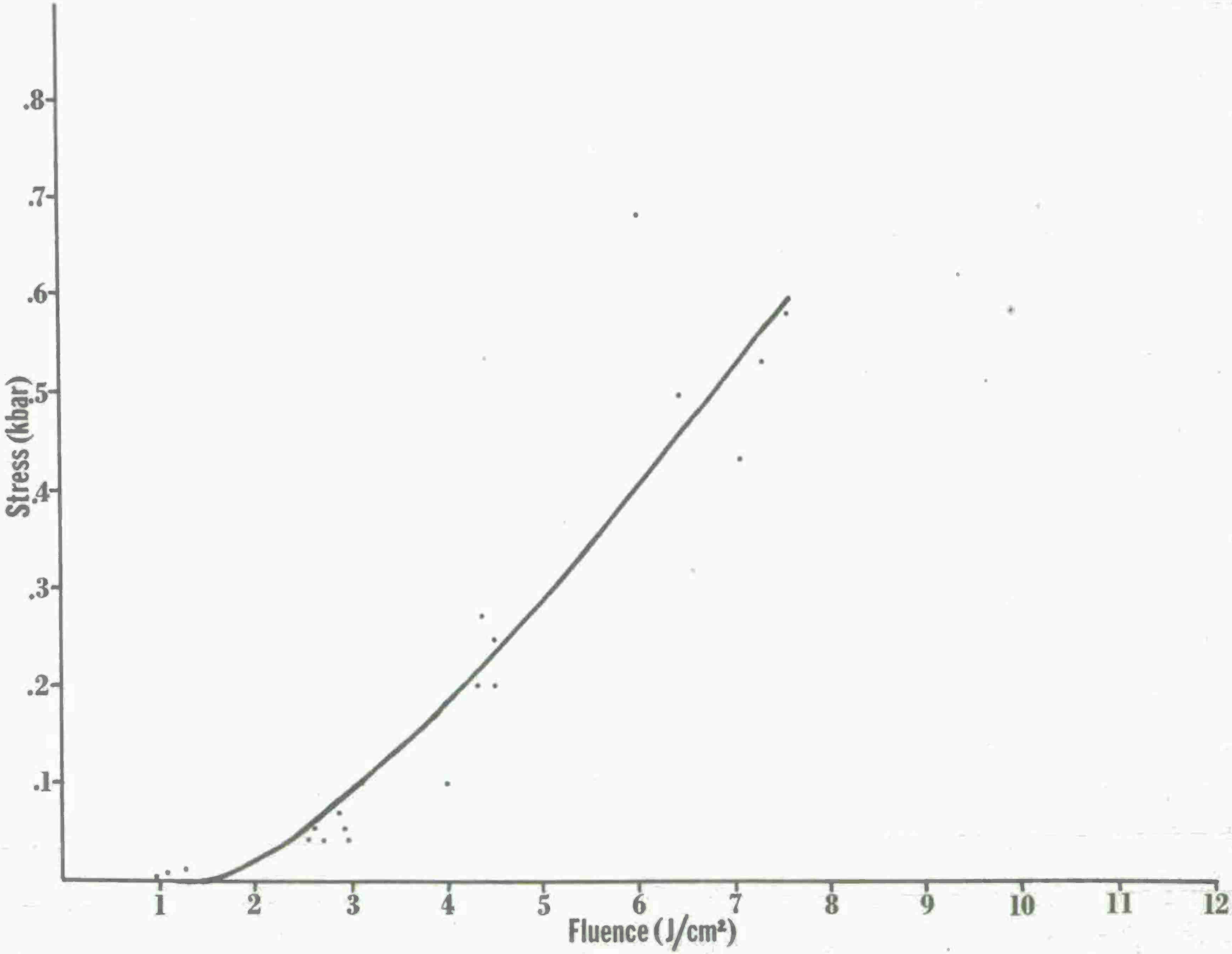

Figure 13. Stress as a function of fluence for uncoated aluminum targets.

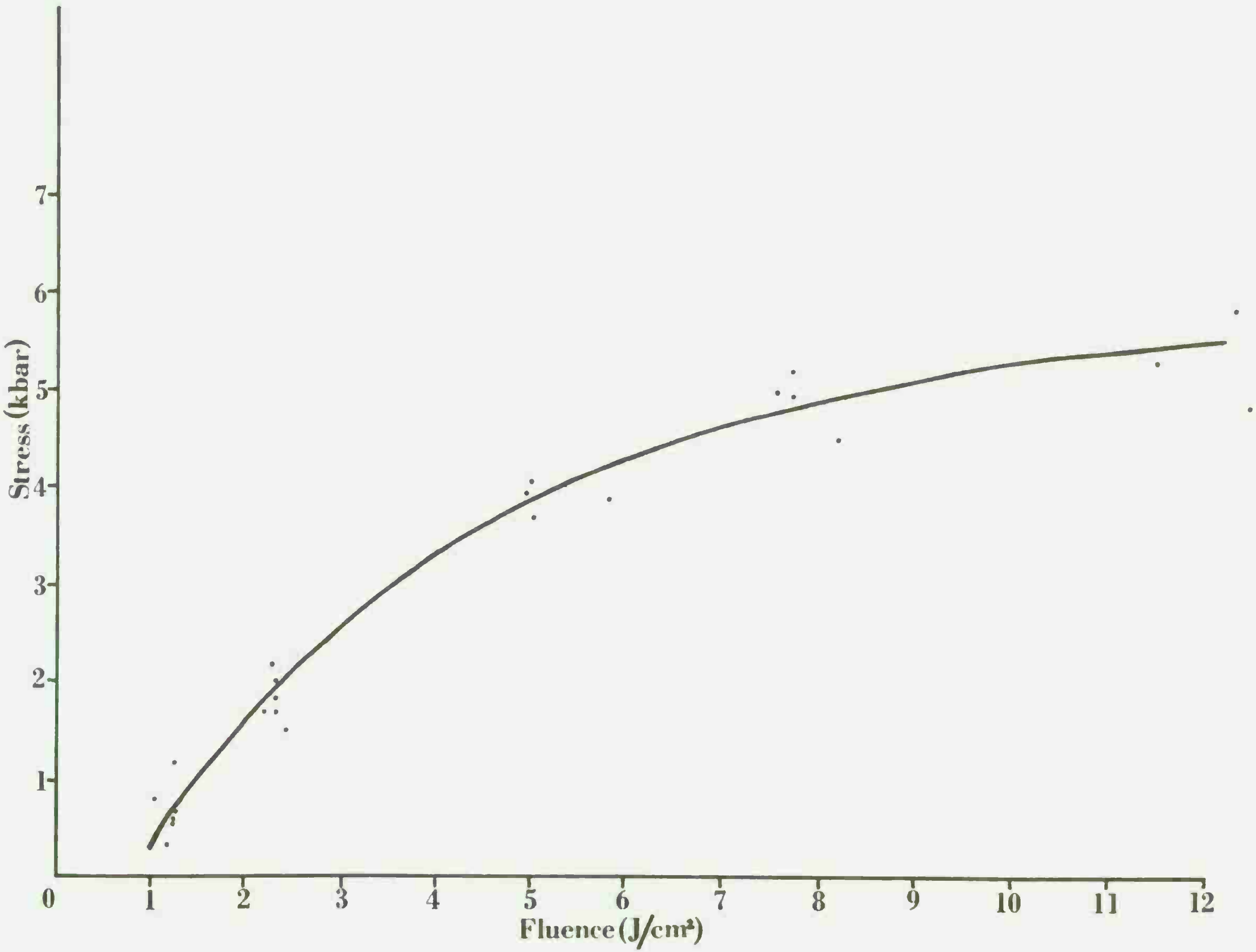

Figure 14. Stress as a function of fluence for targets painted black.

(2) For OD and black, the peak stress increases with paint thickness. This result does not follow the mass-removal results which indicated no increased mass ejected for greater thicknesses. The only other possibility is that the same mass is ejected at greater velocities when the paint is thicker. This possibility indicates a heat conduction effect of the metallic substrate. Obviously, we do not understand this phenomenon adequately, and more work is indicated.

(3) Sufficient data have not been taken yet to provide statistically significant results on the slight apparent difference between the half-widths of the stresses generated in the OD- and black-coated targets. However, one difference is certain: When a sufficient thickness of OD paint is provided (> 2 mils), the compressive main peak is followed by a tensile "tail." A typical oscilloscope trace of this phenomenon is given in Figure 15. The peak of this tensile component comes about 50 nanoseconds

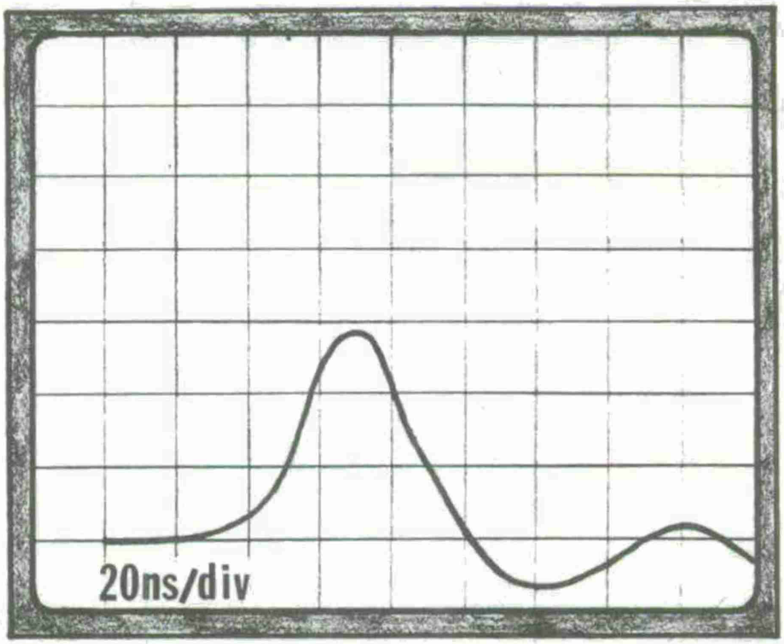

Figure 15. The stress history of a target painted olive drab. Note the presence of the tensile (negative) component.

after the main compressive pulse. This effect is not noted for the black paint and is once again an indication of the greater magnitude of the OD-generated pulse.

(4) A discussion of the white paint results has been purposely deferred until this point. Both black and OD paints are mostly opaque to 1.06-micrometer radiation (OD apparently has a greater skin depth), but white is at least partially transparent.

Thus, one would expect the stress effects to be at least somewhat different. In fact, the difference is apparent simply from the visual appearance of the irradiated target. The white paint shows evidence of both burning (direct coupling) and chipping away (plasma confinement). This dual behavior is also reflected in the oscilloscope presentation of the stress wave (Figure 16). First, the reader should not be concerned with the fact that this stress wave apparently begins about 25 nanoseconds after the OD presentation (Figure 15). This difference is not real; it was caused simply by triggering the oscilloscope internally instead of externally.

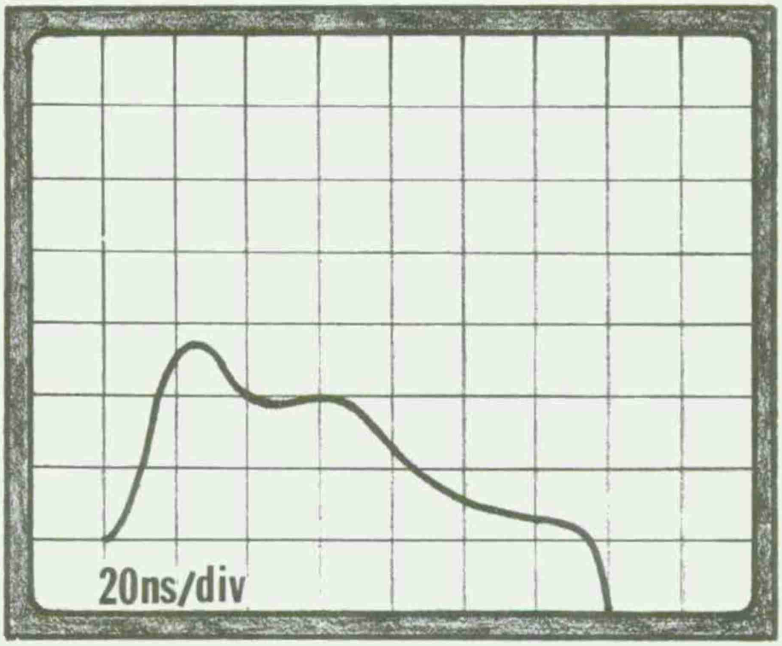

Figure 16. The stress history of a target painted white. Note the presence of the double peaks. (The sudden negative signal at the end signifies merely the end of the writing time of this gage.)

Second, and much more important, note the presence of dual peaks about 30 to 35 nanoseconds apart. This was typical of all the tested white-painted targets having a thickness in the 1- to 2.5-mil range. The separation between the peaks increases from 25 to 50 nanoseconds as the thickness increases. We have devised a model for this behavior. Suppose that part of the radiation couples directly into the paint surface while the rest of the absorbed fraction goes through to the aluminum. This condition would give rise to two separate stress waves–the first caused by plasma trapping, the second caused by direct coupling and delayed by the sound transit time across the paint. The speed of sound in dry paint is not a well-known quantity; but a perusal of the literature reveals that sound speeds for dielectrics of approximately the density of dry paint fall into the 10^5 cm/s-range, which would account for the 25- to 50-nanosecond separation range noted for thicknesses of 1 to 2 mils.

b. **Stress Waves from Combined Paint and Water Coatings.** A few low-fluence ($\sim 1\ J/cm^2$) tests were made using water and paint together. The results are displayed in Table 4.

Table 4. Results Using Combined Paint and Water Coatings

Color	Relative Peak Stress (Arbitrary Units)		Width of Stress at Half-Maximum (Arbitrary Units)	
	With Water	Without Water	With Water	Without Water
White	1	1	1.25	1
Olive Drab	2	1	1.25	1

This means that:

(1) Even though $1\ J/cm^2$ cannot vaporize water, the impulse is still increased, a demonstration of plasma trapping. (Note the increased pulse duration.)

(2) Olive drab must generate more plasma on the surface; thus, the water can trap more plasma.

Although one of the goals of this research was to investigate the effect of laser pulse duration on paint removal and stress production, this portion of the work did not commence until near the end of the test period. The preliminary results are listed in section IV and discussed in Appendix D.

IV. CONCLUSIONS

7. **Conclusions.** Based on the work reported herein, it is concluded that:

a. Laser-induced paint removal is:

(1) Caused by direct coupling (vaporization) or by plasma trapping.
(2) Inversely dependent on pulse duration.
(3) Not a strong function of reflectivity.
(4) Dependent on both absorptivity and skin depth.
(5) More efficient at low fluences ($\simeq 1\ J/cm^2$) than at high fluences (200 to 300 J/cm^2) because of plasma blockage.

b. Experiments with water have shown that:

(1) An H_2O drop vaporizes when exposed to $\simeq 200\ J/cm^2$ (the average intensity is not enough to cause vaporization, but hot spots can cause vaporization).

(2) An H_2O drop is not vaporized by $\simeq 1\ J/cm^2$.

c. Water and/or paint over aluminum, tin, lead, and Plexiglas substrates caused spallation or perforation. Paint thickness can influence spall damage.

d. Stress measurements demonstrated that:

(1) The relative magnitudes of stress and pulse duration given in Table 5 were obtained.

Table 5. Relative Values of Peak Stress and Pulse Duration

Coating	Peak Stress (Relative Value)	Pulse Duration (Relative Value)
Unpainted	1	1
Paint	2	1
Water	4	2
Water and Paint	8	3

(2) Peak pressures as great as 10.5 kilobars with water coating could be obtained.

(3) The shock theory of paint removal is shown invalid by timing experiments.

(4) The stress generated by an OD-covered target is greater than that from a black-painted target. That this follows results from mass-removal experiments and indicates the importance of knowing the skin depth.

(5) White paint acts as both an absorber and plasma trapper (explaining the double-peak stress wave).

(6) Water can be both absorber and plasma trapper. ($1\ J/cm^2$ on a water-coated target increases the stress even though the water is not vaporized.)

e. The following pulse-length phenomena were noted:

(1) Long pulses ($\simeq$ 500 microseconds) can melt through steel but do not remove paint as effectively as do short pulses.

(2) The amount of paint removed must be a function of peak intensity, not of energy.

(3) Shorter pulses (< 1 nanosecond), therefore, probably can cause an equivalent removal of mass at much lower fluences.

V. FUTURE PLANS

8. **Future Plans.** Many data remain to be added in order to form an accurate picture of the phenomenon of coating removal. The most important new area to explore is to determine fluence levels necessary to remove paints with pulses shorter than 1 nanosecond. This line of work certainly could shed some light on the tactical value of a high-energy, short-pulse laser as a coating remover/modifier. This information, together with further work along the same lines as previously followed, can provide the basis for a predictive theory of paint removal. Specifically, the milestones to be accomplished are:

a. **Irradiation with Shorter Pulses.** The existing USAMERDC laser will be modified to produce pulses to less than 30×10^{-12} seconds (30 picoseconds) duration. Because paint removal appears to be a function of peak power rather than of energy density, it is anticipated that this line of research may demonstrate the lower energies which will be required in order to remove paint.

b. **Irradiation Without Substrates.** Because the Teflon method of obtaining large, uniform sheets of paint has proven successful, irradiation of paint samples without substrates will be possible. This will accomplish two things: (1) The direct effect of the substrate itself now can be isolated and analyzed and (2) the properties of the paint alone also can be isolated.

c. **Thickness Removal.** The thickness of paint removed as a function of fluence can now be investigated without the competing effect of the substrate. This investigation will give additional information on paints that are weak absorbers but strong plasma trappers. It also will allow us to isolate and explore further the plasma-trapping effects.

d. **Double Pulse.** The effect of multiple pulses will be determined. Mass removal as a function of pulse separation will be measured.

e. **Theory.** Values of the absorption coefficients will be measured for the various paints. This information taken with data from the above experiments will provide the basis for a predictive, theoretical model for paint removal.

APPENDIX A

ADDITIONAL DATA

A-1 Listing of Paints Used. The paints used in this study are given in Table A-1.

Table A-1. Paint Specifications

Color	Identifying No.	Manufacturer	Federal Specifications
Flat Black	37038	Gard Ind.	TT-L-50F Type I
Red	11105	Strouse, Inc.	TT-L-50E Type I
Orange	12215	Strouse, Inc.	TT-L-50E Type II
Fluorescent Orange	F38903	Day-Glo Color Corp.	TT-L-476
Olive Drab	14064	Strouse, Inc.	TT-L-50E Type I
Field Drab	30118	Vita-Var Co.	TT-E-527-C
Field Drab	VV21012	Vita-Var Co.	None
Forest Green	34079	Vita-Var Co.	TT-E-527-C
Forest Green	21011	Vita-Var Co.	None
Lusterless Olive Drab	X34087	Kerr Chemicals	TT-E-516
Blue	O.T.C.	Kerr Chemicals	None
White	17875	Pacific Aerosols, Inc.	TT-L-50F Type I

A-2 Application. All paints were applied to metallic surfaces cleaned with methanol and allowed to dry at room temperature. The most commonly used substrate was 6061-T6 aluminum, although in a few cases lead was used. Almost all the paints used were directly applied from their original aerosol container. The VV21012 Field Drab and 21011 Forest Green were thinned and brushed. It is, of course, realized that bonding the sprayed paints directly to a substrate is far different than baking the paints after they have been sprayed over an undercoat. The purpose of this research, however, was not to investigate the dependence of bonding but, rather, to explore the interaction between paint and short-pulse laser radiation. As a matter of interest, such baked and undercoated targets were irradiated, and it was found that once again paint could be removed with short-pulse laser radiation. Figure A-1 shows the result of such irradiation.

A-3 Thickness Measurements. At the beginning of this study, extensive measurements were taken of paint thicknesses by means of a Dermitron Model D-5 thickness-measuring instrument. Basically, this device consists of a probe that sends out high-frequency electromagnetic radiation that can induce eddy currents in the metallic substrate beneath the paint layer. By measuring the amount of current detected through the paint and by comparing this with a calibrated dielectric thickness covering a similar substrate,

Figure A-1. The removal of both paint and undercoating from a steel sample irradiated with short-pulse laser energy.

one can then measure the paint thickness. Readings could be taken to 0.01 mil directly. This thickness-measuring device proved to give results that were extremely reproducible, independent of the previous handling of the sample, and independent of the drying time. For example, a blue-painted sample was measured 10 times at nominally the same location (the probe itself is about 5 millimeters in diameter). The results were 0.69 ± 0.03 mil (i.e., an average deviation of 4 percent). It was also found (somewhat to our surprise) that simply spraying the sample gave a coating that was uniform over the area to within about 10 percent. One hundred and five samples were measured, each at least three times, and the results were compared to readings taken with an ordinary micrometer. In every case, the two methods agreed. Thus, although the micrometer could be read directly to only the nearest 0.1 mil, it could be used confidently for routine measurements; indeed, many of our ordinary, day-to-day readings are made this way.

A-4 Spectral Measurements. Virtually all of our spectral information was obtained with a Beckman DK-2A spectrophotometer which is equipped with an integrating sphere for diffuse reflectance and transmittance measurements. Examples of such measurements are seen in Figures A-2 and A-3. (Spectral data have been obtained from nearly all the samples but are not presented here in the interest of brevity.) Also, in order to calculate the absorptivities for the various paints, transmission and reflectance at 1.06 micrometers were measured for various thicknesses. This project has not been completed yet, but the reader may see an example of one such set of data in Figure A-4 (red paint).

A-5 Absorption Measurements. In order to construct a useful theory, not only do we need to know the reflectivity of the paint, but the transmittivity is also an important factor. In point of fact, it is actually the difference between these two quantities, i.e., the absorptivity, that is of importance. It is shown in Appendix B that the fraction of energy present in an electromagnetic wave penetrating a dielectric by a distance z is $e^{-2\alpha z}$, where α is defined as the absorption coefficient for the dielectric. Thus, in order to find out how much energy will be absorbed by a certain type of paint, we must know the absorption coefficient.

Unfortunately, α is not a particularly simple quantity to measure. If we try to measure the transmission of 1.06-micrometer light with the spectrophotometer, we must coat a piece of transparent material. Allowir . for the absorptivity of the substrate itself poses no particular problem, but then one must calc· ·te the losses at the paint/ substrate interface. From electromagnetic theory, the reflecta. : R at an interface between medium 1 and medium 2 is:

$$R = \left[\frac{1 - n_2/n_1}{1 + n_2/n_1}\right]^2,$$

where $n_{1,2}$ = index of refraction of medium 1,2.

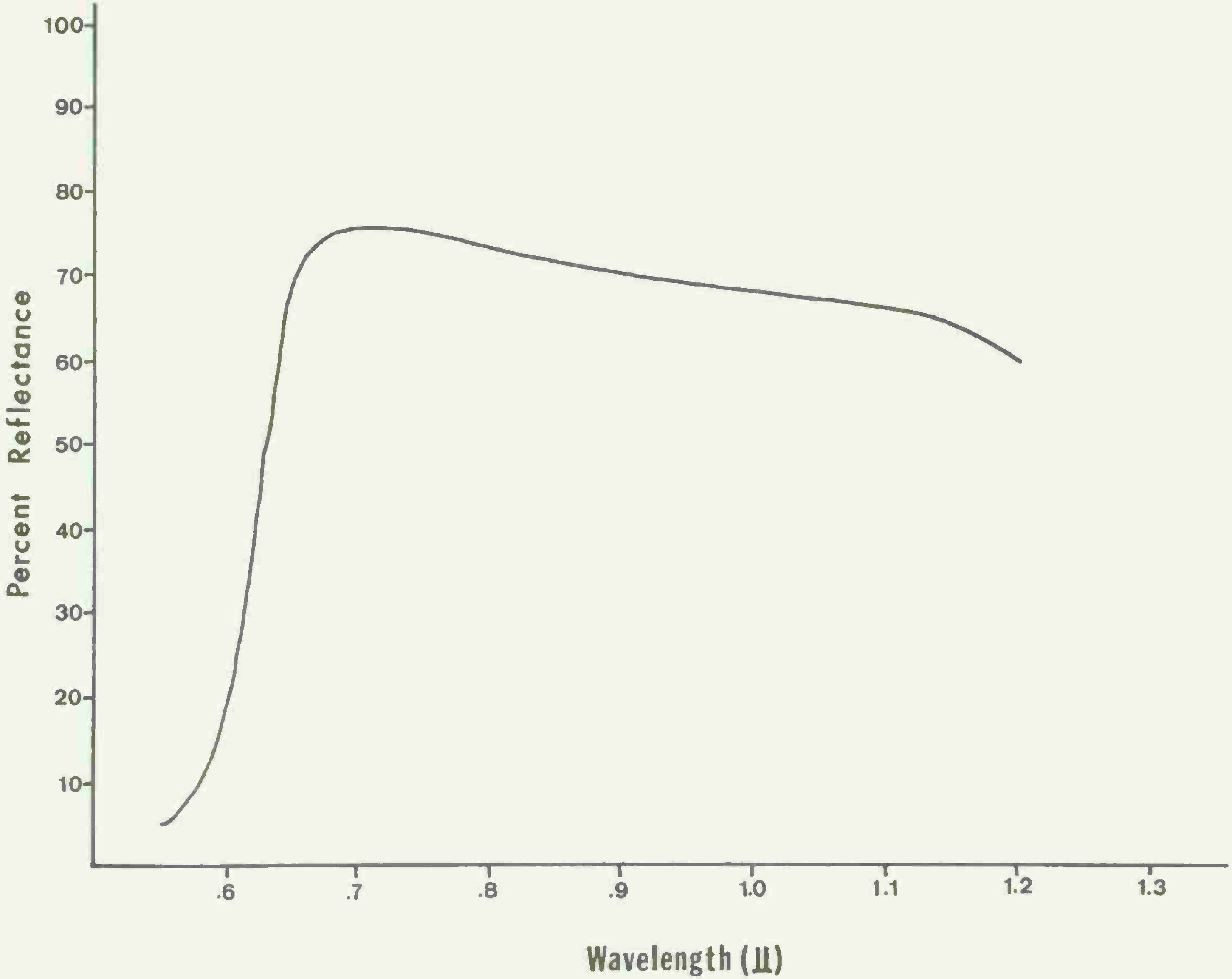

Figure A-2. The reflectance of a red-paint sample for the 0.6- to 1.2-micrometer band.

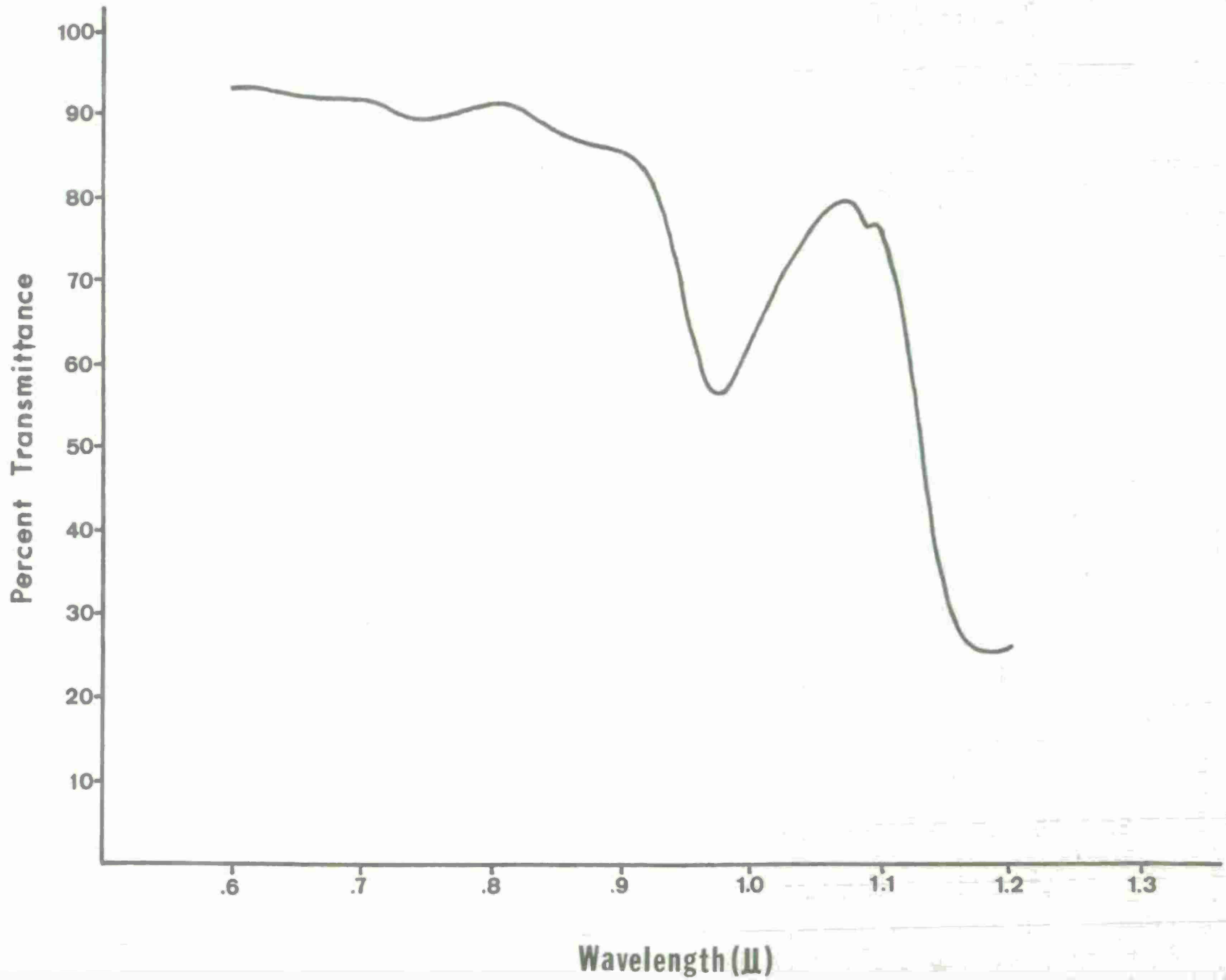

Figure A-3. The transmission of a water sample (1.0 centimeter thick) for the 0.6- to 1.2-micrometer band.

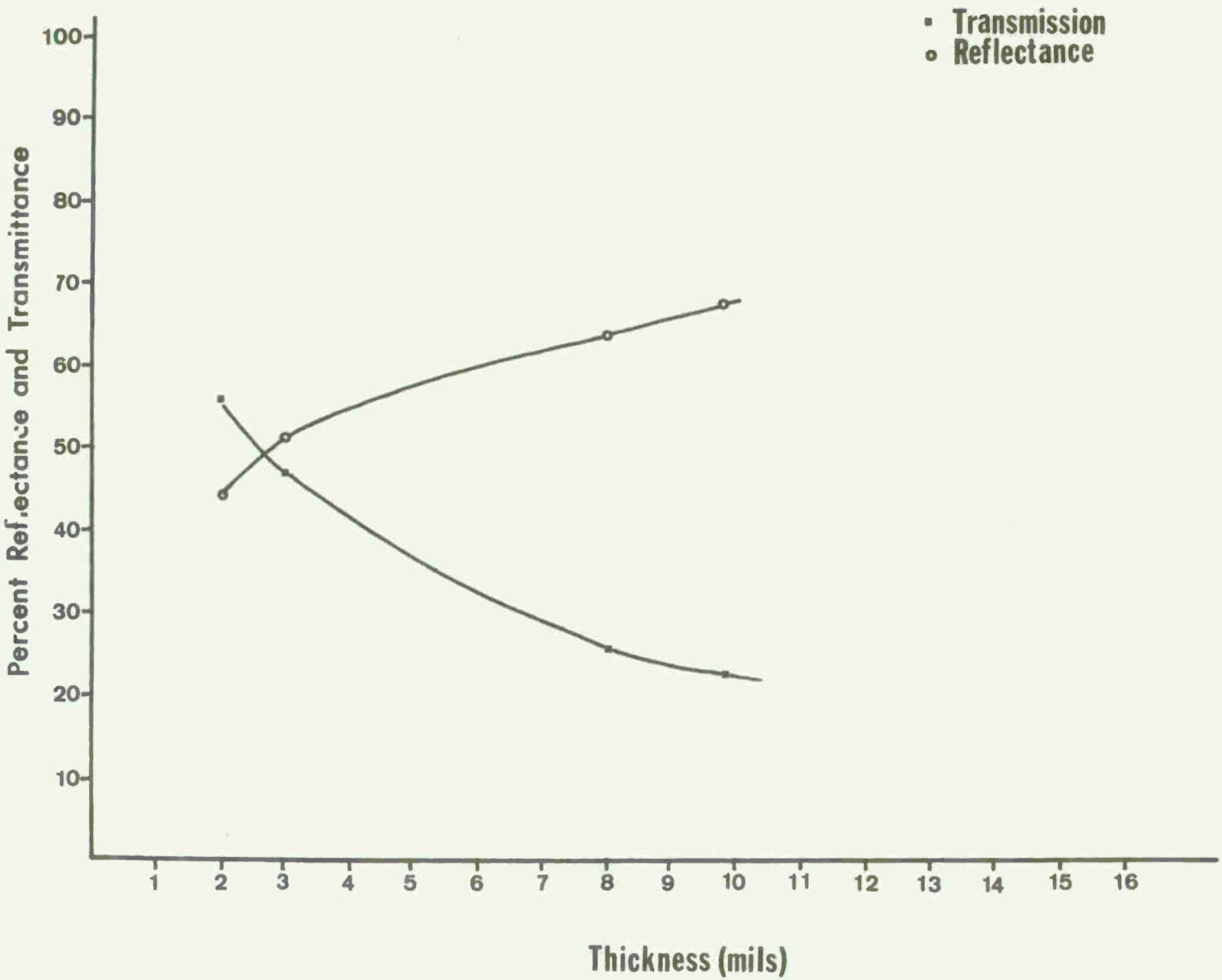

Figure A-4. The transmission and reflectance at 1.06 micrometers of a few thicknesses of red paint.

Measuring the index of refraction of dry paint is no simple matter. Fortunately, we were able to devise a technique which obviated the need for such a measurement.

One of the well-known properties of tetrafluoroethylene (Teflon) is that few substances adhere well to its surface. We have discovered that most of our paint samples also will not adhere well to Teflon. When a Teflon-coated sheet of aluminum (cookie sheet) is sprayed with paint, it is possible to peel up enough of a paint sheet (1-inch square) to mount in the spectrophotometer and, thus, to measure the transmission and reflectance. Only a few preliminary measurements have been made thus far. They are presented in Table A-2.

Table A-2. Transmission and Reflectance for Paint Samples

Color	Thickness (Mils)	Transmission (Pct)	Reflection (Pct)	Absorption (Pct)
Red	7.8	25.5	63.5	11.0
Red	9.6	22.8	62.6	14.6
Black	1.7	0.	3.0	97.0
Black	2.2	0.	3.0	97.0
Black	4.5	0.	3.0	97.0
White	4.4	5.4	78.5	16.1
White	12.3	0.	80.4	19.6
Orange	3.6	13.5	61.9	24.6
Orange	7.7	1.9	65.5	32.6
Glossy OD	0.8	17.1	7.8	75.1
Glossy OD	2.2	0.	6.9	93.1
Lusterless OD	6.5	0.	7.8	92.2
Field Drab	4.3	1.5	54.5	44.0
Field Drab	4.5	0.	53.8	46.2
Forest Green	6.4	0.	33.4	66.6

Obviously, many more data are needed before accurate values of α can be computed, but the implication seems clear. The absorptivity of paint can be measured for various thicknesses using this method. From these absorptivities, the effective skin depth can be calculated. Skin depth might well prove to be the important factor in predicting how much paint can be removed with a given fluence.

For example, consider paint samples 1 and 2 with skin depths $\delta_1 > \delta_2$ (i.e., most of the laser energy is deposited in a thicker layer in sample 1 than in sample 2). Assuming that paint vaporization takes place in both cases, we see that more mass will be removed from sample 1 than from sample 2, and this may be true even if the reflectivity of sample 2 is less than sample 1. More research is needed to establish this point.

APPENDIX B

LASER SPECIFICS

B-1 Description of Laser System. The Korad K-2 laser oscillator used for these experiments is a Q-switched device essentially consisting of a neodymium-doped glass rod, a xenon flash tube and reflector, a Pockels cell, and a high-voltage power supply and capacitor bank. When the laser is in operation, the high voltage (6 to 10 kV) is used to charge the capacitors which fire the flashlamp, thus pumping up the energy levels of the rod. The Pockels cell is then activated after an appropriate delay (usually 700 to 800 microseconds) in order to assure maximum short-pulse output. A reproduction of a photodiode recording of an actual pulse is given in Figure B-1. Typical performance specifications follow:

Energy (J)	0–10
Pulse Duration (ns)	20–30
Wavelength (μm)	1.06
Peak Power (W)	$0–5 \times 10^8$

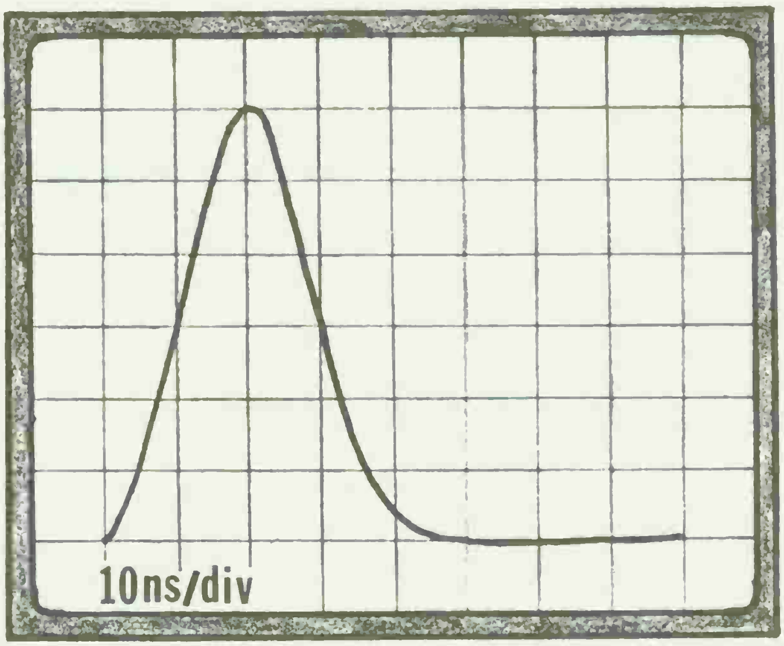

Figure B-1. Photodiode recording of a typical 20-nanosecond laser pulse.

The laser can be operated without the Pockels cell by suitable reflector replacement. If this is done, then the following parameters are achievable:

Energy (J)	120
Pulse Width (μs)	500
Peak Power (W)	2.4×10^5

A unique characteristic of this laser is the ability to obtain two pulses with a variable separation. In this mode, the parameters are:

Energy Per Pulse (J)	4
Pulse Width (ns)	30
Separation Between Pulses	0 to 500 μs in increments as small as 10 ns

This extremely useful property is obtained by optically splitting the rod into upper and lower halves by means of a prism placed between the rod and the Pockels cell at a height equal to one half the rod diameter. Thus, one-half of the light goes to one Pockels cell, and the remaining part is shunted off to another cell. The firing of these cells with respect to one another is then delayed, and this provides the separation.

This double-pulse capability is unique with our laser (for these high energies) and will enable us to investigate multipulse effects on coated surfaces in the future.

B-2 Energy and Fluence Measurements. The energy standard for measuring laser radiation in this laboratory is a calibrated, Korad KJ calorimeter with an accuracy of ± 5 percent. Since this instrument requires approximately 1 hour to cool down after a shot, it is used only to calibrate our secondary measuring devices, such as photodiodes. At any rate, the energy is monitored for every shot. The overall estimated error for energy measurements is ± 10 percent.

Measuring the fluence poses a special problem for small-diameter spots. Consider Figure B-2, where R is the radius of unfocused laser light and f is the focal length of the lens.

From the diagram,

$$\frac{R}{f} = \frac{r}{y}\text{, thus}$$

$$r = \frac{Ry}{f}.$$

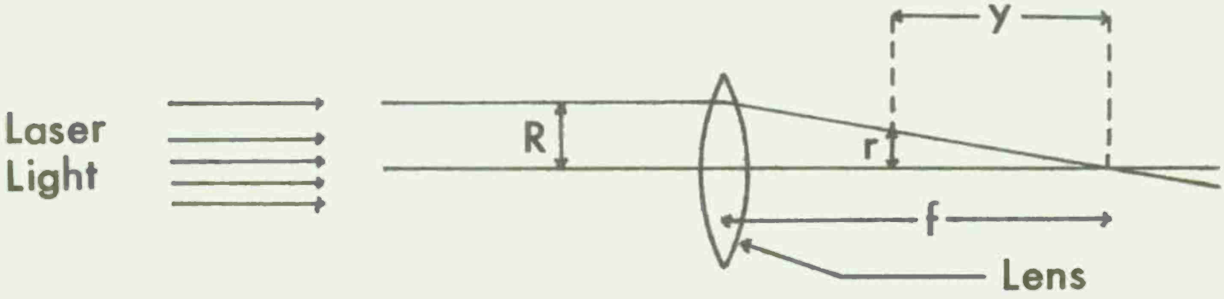

Figure B-2. Lens geometry.

So the area of a spot with radius r is:

$$A = \pi \left(\frac{Ry}{f}\right)^2.$$

Thus, the fluence F (energy per unit area) is:

$$F = \frac{E}{\pi}\left(\frac{f}{Ry}\right)^2$$

In principle, this is all there is to measuring the fluence at some point. The quantities E, f, R, and y are directly measurable. In practice, however, the direct measurement of f proves to be difficult because of chromatic aberration in the lens. It is a straightforward process to take a collimated light source (say a He–Ne laser) and find the focal length by inspection; however, light of 1.06 micrometers wavelength will not, in general, focus at the same point. There is evidence that this difference may be as large as 5 percent for the short-focal-length (200-millimeter) lenses we commonly use. In order to reduce this error, light-sensitive paper (so-called "burn" paper) is used to determine the focal plane with 1.06-micrometer radiation. The laser pulse is focused onto the paper and leaves an approximately circular pattern. The position of the paper is then changed on the optical bench until a minimum spot size is observed. This position can be identified as the focal point. Unfortunately, this method also has its inherent flaws. Since the beam is energetically and optically nonuniform, the position of minimum spot size can be ill defined. Moreover, because of divergence effects, the entire concept of a single location for the minimum spot size is somewhat incorrect. Actually, there exists a minimum focal volume, the depth of which is dependent on the laser divergence, mode structure, and lens focal length. For this reason, the above methods are supplemented by observation of air breakdown. The energy of the laser is varied until the minimum necessary to cause air breakdown is established, and the position of this event is recorded photographically. This information, together with the above, is used to find the focal plane.

All of the before-mentioned difficulties offer little or no problem to low-fluence measurements. Only the small diameters are sources of great potential error. The following error estimates reflect this fact:

Fluence (J/cm^2)	Estimated Error (Pct)
0–50	20
50–100	25
100–300	35
>300	>35

Still, for the purpose of this investigation, these are not large errors since the same spot sizes are used and only comparative fluences are important.

APPENDIX C

CALCULATION OF ABSORPTIVITY

In encountering many practical problems dealing with the passage of electromagnetic radiation through matter, the engineer often must calculate how much energy is remaining after the energy traverses a certain thickness of attenuator. It is the purpose of this appendix to sketch the development of such a calculation. This is certainly not an original proof but is intended solely to refresh the memory of the reader.

Assume that we are dealing with a simple dielectric in which the electrons are bound to the atoms. If an electromagnetic wave acts on these charges, it can cause them to oscillate about the equilibrium position. If we consider these bound charges as classical damped harmonic oscillators, the differential equation of motion is:

$$m \frac{d^2 \vec{r}}{dt^2} + m\gamma \frac{d\vec{r}}{dt} + K\vec{r} = -e\vec{E},$$

where: m, e = mass and charge respectively, of the electron,

$\vec{E}$ = instantaneous magnitude of the electric field,

γ = frictional damping constant,

K = force constant, and

$\vec{r}$ = displacement of electron from equilibrium.

If the electric field varies harmonically as $e^{-i\omega t}$, where ω is the frequency of the field, and if the polarization P is defined as $-Ne\vec{r}$, where N is the number of electrons per unit volume, then the instantaneous polarization is:

$$\vec{P} = \frac{Ne^2}{-m\omega^2 - i\omega m\gamma + K} \vec{E}.$$

From Maxwell's equations and the assumed linear relationship between $\vec{P}$ and $\vec{E}$, this is easily seen to give:

$$\nabla^2 \vec{E} = \frac{1}{c^2}\left(1 + \frac{Ne^2}{m\epsilon_o} \frac{1}{\omega_o - \omega^2 - i\gamma\omega}\right) \frac{\partial^2 \vec{E}}{\partial t^2},$$

where: c = speed of light,
ω_o = resonant frequency of bound electrons, and
ϵ_o = permittivity of free space.

The solution to this differential equation is:

$$E = E_o \, e^{-\alpha z} \; e^{i(kz-\omega t)},$$

where: k = complex wave number = $K' + i\alpha$, and

$\alpha = \frac{\omega}{c} L$, where L is the complex part of the index of refraction.

Since the energy U in the wave is proportional to $E^* E$, then

$$U = U_o \; e^{-2\alpha z},$$

which is the desired result.

APPENDIX D

LONG-PULSE MEASUREMENTS

One of the goals of this research was to compare the effects at long-pulse (LP) durations (> 100 microseconds) with the short-pulse (SP) effects. Unfortunately, the coupling optics did not arrive until late in the fiscal year; so, extensive measurements were not made. However, preliminary results are available, and they show the following:

a. Up to 120 joules can be delivered to a target in a pulse having a half-width of 500 microseconds. When this energy is focused, 1/8 inch of steel can be melted with one pulse.

b. The amount of paint removal with an LP is negligible compared to SP removal (equal fluences).

c. The amount of stress generated with an LP is negligible compared to SP generation (equal fluences).

d. The short pulse of our laser is nominally of a 20- to 25-nanosecond duration. It can be lengthened to 40 to 50 nanoseconds by suitably adjusting the optical cavity and the Pockels cell. When this was done, once again, greatly reduced paint removal and stress generation were observed.

Conclusions concerning pulse widths:

a. Paint removal is probably a function of peak intensity, not fluence.

b. The above information implies that paint removal might be increased by going to shorter pulses; i.e., the same effects can be obtained at much lower fluences. For example, if a certain amount of paint removal is possible at 3 J/cm^2 with a 30-nanosecond irradiation, then the same removal might be effected at 0.003 J/cm^2 with a 30-picosecond pulse. Such pulse generation is well within the state of the art.

DISTRIBUTION FOR USAMERDC REPORT 2138

No. Copies	Addressee
	Department of Defense
1	Director, Technical Information Defense Advanced Research Projects Agency 1400 Wilson Blvd Arlington, VA 22209
1	Director Defense Nuclear Agency ATTN: STTL Washington, DC 20305
12	Defense Documentation Center Cameron Station Alexandria, VA 22314
	Department of the Army
7	Commander US Army Materiel Command ATTN: AMCRD-WB AMCRD-T AMCRD-J AMCRD-O AMCRD-G AMCRD-FP AMCDL 5001 Eisenhower Ave Alexandria, VA 22333
1	Commander US Army Troop Support Command ATTN: AMSTS-K 4300 Goodfellow Blvd St. Louis, MO 63120
1	Commander HQ, TRADOC ATTN: ATEN-ME Fort Monroe, VA 23651
1	HQDA (DAMA-AOA-M) Washington, DC 20310
1	HQDA (DAEN-RDL) Washington, DC 20314
1	US Army Research Office Physical Sciences Div ATTN: Dr. R. Watson Washington, DC 20310
1	HQDA (DAEN-MCE-D) Washington, DC 20314
3	Commander US Army Missile Command ATTN: AMSMI-RR Redstone Arsenal, AL 35809
2	Commander Rock Island Arsenal ATTN: SARRI-LPL Rock Island, IL 61201
1	Director Army Materials and Mechanics Research Center ATTN: AMXMR-STL, Technical Library Watertown, MA 02172
2	Commander US Army Natick Laboratories ATTN: Technical Library STSNL-VMC (Dr. Healey) Natick, MA 01760
1	U.S. Army Ballistic Research Labs Technical Library AMXBR-LB (Bldg 305) Aberdeen Proving Ground, MD 21005
2	Commander Edgewood Arsenal ATTN: SAREA-TS-L Aberdeen Proving Ground, MD 21010
1	Commander US Army Aberdeen Proving Ground ATTN: STEAP-MT-U (GE Branch) Aberdeen Proving Ground, MD 21005
1	Director US Army Materiel Systems Analysis Agency ATTN: AMXSY-CM Aberdeen Proving Ground, MD 21005
1	Director US Army Engineer Waterways Experiment Station ATTN: Chief, Library Branch Technical Information Ctr Vicksburg, MS 39180
1	Commander Picatinny Arsenal ATTN: SARPA-TS-S No. 59 Dover, NJ 07801

No. Copies	Addressee
1	Plastics Technical Evaluation Center Picatinny Arsenal, Bldg 176 ATTN: A. M. Anzalone SARPA-FR-M-D Dover, NJ 07801
2	Commander White Sands Missile Range ATTN: STEWS-LG-EC (Mr. Paul Moreau) White Sands Missile Range, NM 88002
2	Commander Frankford Arsenal ATTN: Library, K2400, Bl 51-2 Philadelphia, PA 19137
1	Learning Resources Center US Army Engineer School Bldg 270 Fort Belvoir, VA 22060
1	Commander US Army Electronics Command ATTN: AMSEL-GG-TD Fort Monmouth, NJ 07703
1	President US Army Aviation Test Board ATTN: STEBG-PO Fort Rucker, AL 36360
	USAMERDC
1	Commander Technical Director Assoc Tech Director (R&D) Chief, Legal Office CIRCULATE
1	Chief, Lab 1000 Chief, Lab 2000 Chief, Lab 3000 Chief, Lab 4000 Chief, Lab 5000 Chief, Lab 6000 Chief, Lab 7000 Chief, Lab 8000 Chief, Tech & Res Spt Ofc CIRCULATE
5	Lab 5000
25	Countersurv & Topo Div
2	Tech Reports Ofc
3	Security Ofc
2	Tech Documents Ctr

No. Copies	Addressee
1	Requirements and Programs Ofc
1	Information Ofc
1	Legal Ofc
	Department of the Navy
2	Director, Physics Program (421) Office of Naval Research Arlington, VA 22217
3	Director Naval Research Laboratory ATTN: Code 2627 Washington, DC 20375
1	Director Earth Physics Program Code 463 Office of Naval Research Arlington, VA 22217
	Department of the Air Force
1	HQ USAF/RDPS (Mr. Allan Eaffy) Washington, DC 20330
3	AFWL (DEZ-S) Kirkland AFB, NM 87117
1	AFAPL/SFL Wright-Patterson AFB, OH 45433
1	ASD/ENCSP Wright-Patterson AFB, OH 45433
	Others
1	Professor Raymond R. Fox School of Engineering and Applied Science The George Washington University Washington, DC 20052

DEPARTMENT OF THE ARMY
U. S. ARMY MOBILITY EQUIPMENT
RESEARCH AND DEVELOPMENT CENTER
FORT BELVOIR, VIRGINIA 22060

OFFICIAL BUSINESS
PENALTY FOR PRIVATE USE, $300

POSTAGE AND FEES PAID
U. S. DEPARTMENT OF THE ARMY
DOD-314

U.S.MAIL

THIRD CLASS MAIL